Acta Geologica Polonica, Vol. 75 (2025), No. 1, e33
DOI: 10.24425/agp.2024.151755

Petrology, mineral chemistry and geochemistry of chloritite associated with Neoproterozoic ophiolitic ultramafics in the Eastern Desert of Egypt, Arabian-Nubian Shield

BASSAM A. ABUAMARAH[1], AMANY M.A. SEDDIK[2], MOKHLES K. AZER[3], OMAR BARTOLI[4] and MAHMOUD H. DARWISH[2]

[1] *Department of Geology and Geophysics, King Saud University, Riyadh 11451, Saudi Arabia; e-mail: babuamarah@ksu.edu.sa*
[2] *Geology Department, Faculty of Science, New Valley University, El-Kharga, 72511 Egypt; e-mails: amanyseddik7@gmail.com; mahmoud.hamed68@sci.nvu.edu.eg*
[3] *Geological Sciences Department, National Research Centre, Cairo, Egypt; e-mail: mokhles72@yahoo.com*
[4] *Geoscience Department, University of Padova, Padova, Italy; e-mail: omar.bartoli@unipd.it*

ABSTRACT:

Abuamarah, B.A., Seddik, A.M.A., Azer, M.K., Bartoli, O. and Darwish, M.H. 2025. Petrology, mineral chemistry and geochemistry of chloritite associated with Neoproterozoic ophiolitic ultramafics in the Eastern Desert of Egypt, Arabian-Nubian Shield. *Acta Geologica Polonica*, **75** (1), e33.

This study presents for the first time, the field observations, petrography, mineral chemistry and geochemistry of chloritite hosted in the Al-Barramiya Neoproterozoic ophiolite of the Eastern Desert of Egypt, Arabian-Nubian Shield (ANS). The Al-Barramiya ophiolite is one of the most important ophiolitic sequences exposed in the ANS. It is affected by different types of alterations including carbonatization, listvenitization, chloritization and rodingitization. The Al-Barramiya chloritite occurs as thin layers associated with highly serpentinized peridotite. It is a fine-grained rock entirely composed of chlorite (85–95 vol.%) with minor talc and accessory minerals (epidote, rutile, titanite, corundum and opaque minerals). The chlorite minerals in the chloritite are represented mainly by diabantite, while those in the serpentinites include ripidolite. Depending on the chemical composition of the chlorites, the chlorite in chloritite formed at temperatures ranging between 200 and 250°C, which are lower than those of the disseminated chlorite in the serpentinite (310–345°C), indicating their formation in different hydrothermal stages. The chloritite samples are rich in total REE contents (17.9–27.3 ppm) compared with the associated serpentinites (0.69–0.87 ppm). They are characterized by slightly depleted LREE relative to HREE [(La/Lu)n = 0.8–0.9], with a moderately negative Eu-anomaly [(Eu/Eu*)n = 0.4–0.5]. The negative Eu-anomalies are derived from chloritization fluids or reflect the presence of talc in the chloritite. Based on field work, petrography, mineralogical and geochemical data, the studied chloritite has been interpreted as being derived from the associated serpentinized ultramafics by hydrothermal alterations. This is supported by an enrichment of chloritite in compatible trace elements (Cr = 2031–2534 ppm, Ni = 1264–1988 ppm, Co = 76–101 ppm) similar to that which is observed in the associate serpentinite.

Key words: Arabian-Nubian Shield; Al-Barramiya ophiolite; Chloritite; Chloritization; Fore-arc setting.

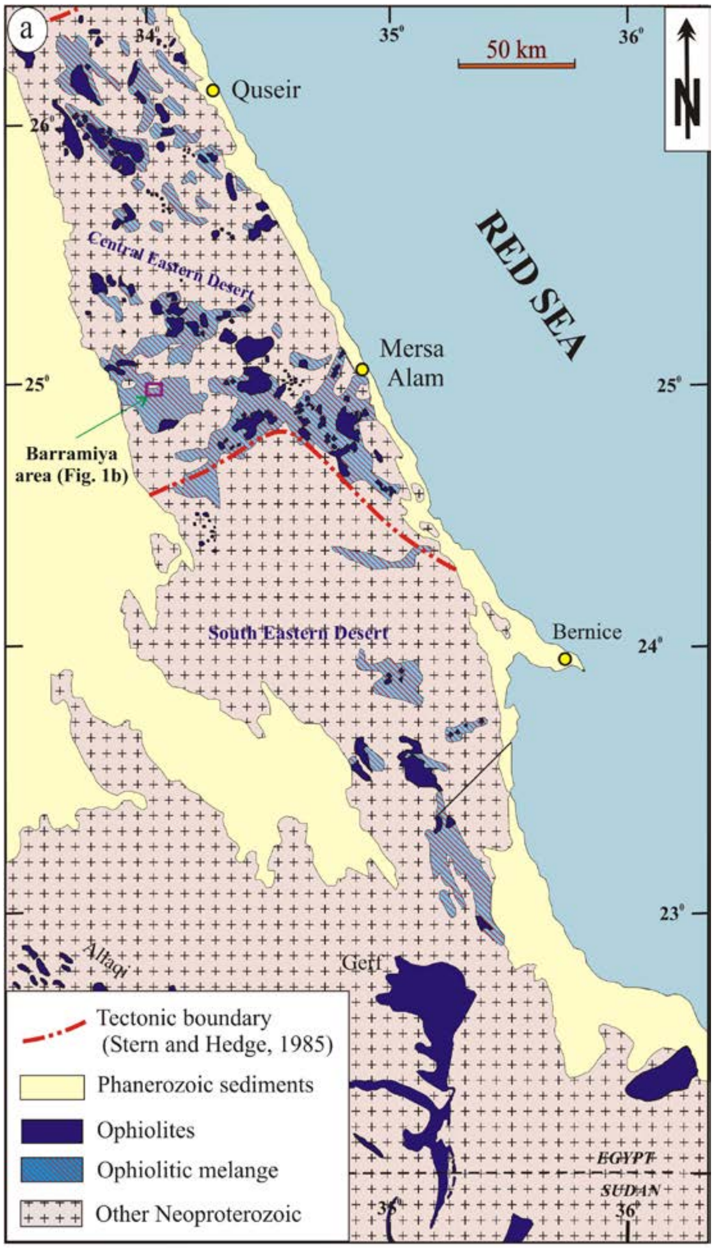

Text-fig. 1. Geologic maps: (a) regional geologic map showing the distribution of ophiolitic rocks in the Eastern Desert of Egypt (modified after Shackleton 1994). The location of figure 1b is indicated, and (b) detailed geological map of the study area.

INTRODUCTION

The ultramafic rocks associated with the Arabian-Nubian Shield (ANS) ophiolites are generally highly altered and transformed into serpentinite or a mixture of serpentine, talc, tremolite, magnesite, chlorite, magnetite, and carbonate (Stern *et al.* 2004; Ali *et al.* 2010). To date, it is unclear whether this alteration occurred before, during, or after the emplacement. The term chloritite generally refers to chlorite-rich rocks that result from intense hydrothermal alteration of both mafic and ultramafic rocks (Kotschoubey *et al.* 2016; Compagnoni *et al.* 2021). It is a monomineralic dark green rock composed of mostly chlorite and minor opaque minerals. The chlorite originated either from ultramafic rocks by metasomatism or rarely from pelitic sediments by low grade metamorphism (Abdel-Karim 2000).

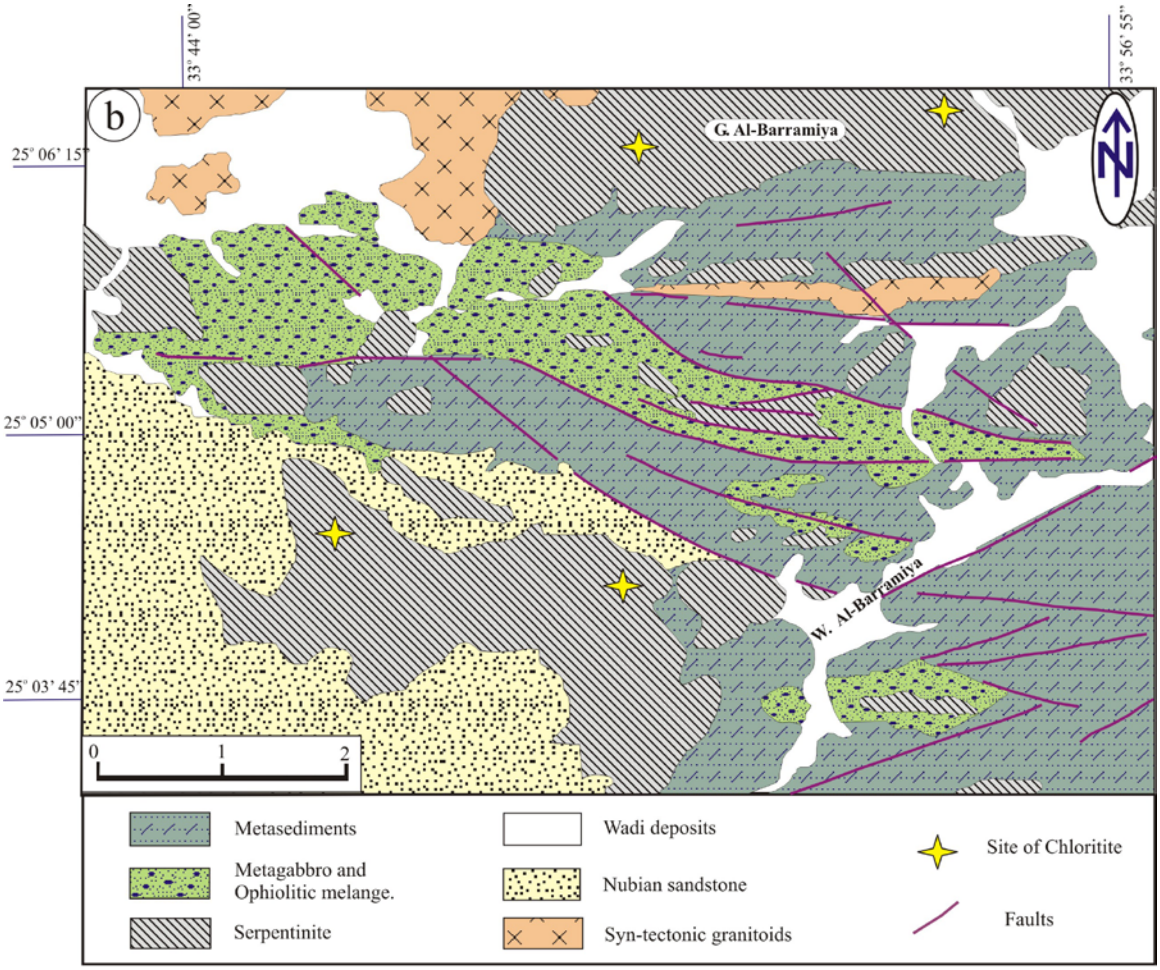

Text-fig. 1. (*continued*).

In the ANS, the chloritite is found in association with the altered ophiolitic ultramafic rocks as thin layers around serpentinites or as narrow dark bodies around rodingites (Mubarak *et al.* 2020; Gahlan *et al.* 2021; Abuamarah *et al*. 2023). The serpentinized ultramafics and associated chloritite in the ANS are regionally significant in the context of this shield and globally significant as an example of alteration processes that affected the Proterozoic continental crust.

Most chloritites in the Eastern Desert of Egypt have been considered as ortho-schists derived from serpentinized ultramafic rocks (Takla and Noweir 1980) or as para-schists corresponding to the geosynclinal metasediments (Akaad and Noweir 1980). Recently, Takla *et al.* (1991) classified the chloritites in the Nubian Shield into three types. The first is rich in sheridanite and formed after serpentinized ultramafic masses, the second is ripidolite-rich and formed after metapyroxenite and the third type is rich in corundophyllite associated with metasediments.

The Neoproterozoic ophiolites of the Al-Barramiya District represent an outstanding example of the ophiolites of the northwestern corner of the ANS. They are dismembered ophiolites which are strongly deformed and metamorphosed. No petrological or geochemical studies on the exposures of chloritite occurring in the Al-Barramiya area have been carried out before. Therefore, the nature and origin of the Al-Barramiya chloritite and the associated ultramafics are investigated in this work, providing additional information for a more complete petrologic overview of the ophiolitic rocks of the northwestern corner of the ANS. This work presents field observations, petrographic description, mineral chemistry and whole rock chemistry of chloritites and associated serpentinites in the Al-Barramiya area in the Eastern Desert of Egypt. Also, the fresh relics of primary mantle minerals such as Cr-spinel are used to place constraints on the early history of the ANS arc-accretionary phase.

GEOLOGIC SETTING AND FIELD OBSERVATIONS

The area under investigation represents a part of the most famous exposure of ultramafic rocks in the Eastern Desert of Egypt which is known as the Al-Barramiya ophiolite. It is located in the Central Eastern Desert (Text-fig. 1a). The mapped area is mainly covered by ophiolites, island-arc assemblages and intrusive rocks (Text-fig. 1b). Ophiolitic rocks comprise mainly serpentinized peridotite, metagabbro and ophiolitic mélange. The ophiolitic mélange consists of various rock fragments with different sizes embedded in a foliated matrix of metasedimentary rocks. The serpentinite masses are the most common rock fragments in the ophiolitic mélange with subordinate metagabbros, metavolcanics and metasediments. Most serpentinite masses occur as thrust sheets which are elongated in a general ENE-WSW trend concordant with the foliation direction in the surrounding matrix of the ophiolitic mélange.

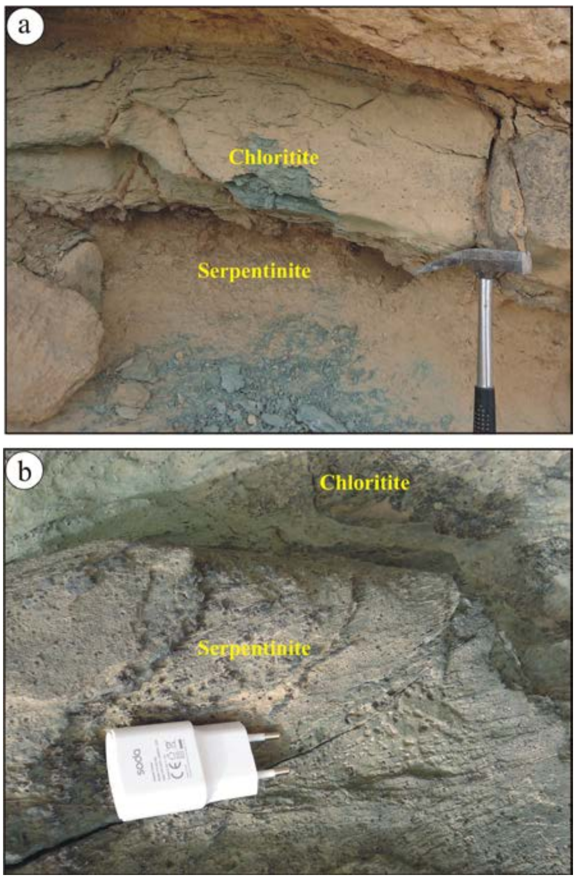

Text-fig. 2. Field photographs: (a) chloritite developed between serpentinized ultramafics and talc-carbonates and (b) chloritite developed along the peripheries of the serpentinized ultramafics.

Along shear zones and thrust faults, serpentinites are altered to talc-carbonate, listvenite and magnesite. The talc-carbonate rocks are massive or schistose, and range in color from creamy white to light grey to yellowish-white or buff. Magnesite is observed as nodules, irregular pockets and veinlets in the sheared ultramafic rocks and talc-rich rocks which are concordant with the foliation in the host rocks. Listvenite occurs as irregular masses and ridges of reddish brown color. It forms high relief relative to its country rocks and shows a porous texture as the result of supergene oxidative weathering. Locally, many fractures filled with carbonate veinlets and quartz ribbons are observed in the sheared listvenite. Metagabbro occurs as allochthonous irregular masses that locally overly the serpentinites and show spheroidal weathering. The island-arc rocks include metavolcanics, metasediments and metagabbros. The intrusive rocks in the study area are represented mainly by granodiorite and monzogranite. They intrude serpentinites and adjacent island arc rocks with a sharp intrusive contact.

The investigated chloritite is commonly developed along the peripheries of the ultramafic masses (Text-fig. 2a, b). It occurs as a continuous layer (thickness of 10–30 cm) at the outer margins and along the fractures of sheared ultramafic bodies. The chloritite comprises a fine-grained and massive rock with grayish green to dark green colour. Locally, it is stained by the reddish brown colour of hematite.

ANALYTICAL METHODS

For the petrographic analyses, some thin sections of the most representative collected samples were prepared. Mineral assemblages and textures were examined in order to characterize mineralogical compositions, grade of metamorphism and the nature of the alteration. These thin sections were examined using a polarizing microscope (Nikon) equipped with a digital photomicrographic attachment**.** Based on the examined thin sections, some polished slabs of the representative samples were prepared and studied using reflected light under the same microscope for identifying the ore minerals and their characteristic textures.

Some essential and accessory minerals were analyzed in both chloritite and serpentinites using an electron microprobe. The analyzed minerals include chlorite, mica, chrome spinel, magnetite, Cr-magnetite, ferritchromite, ilmenite, brookite, epidote and apatite. Mineral chemical analyses were obtained from polished thin-sections using the JEOL JXA-8530F field-emission electron microprobe (EMPA) housed at the Department of Earth Sciences, University of Western Ontario, Canada. Operating conditions were 20 kV probe current, 40–60 nA beam current, 1–2 µm diameter beam, counting time of 5–10 s and a ZAF matrix correction routine program applied. A set of natural and synthetic mineral standards were used for calibration. The standards were orthoclase for K, albite for Na and Al, anorthite for Ca, rutile for Ti, zircon for Si, forsterite for Mg and fayalite for Fe. Calculations of cations in the structure of the analyzed minerals were done using Excel sheets and Minpet software program. The mineral formulae were normalized to certain oxygens depending on each mineral as atom per formula unit (a.p.f.u.).

Based on the petrographic study, 9 samples were selected out of 21 for chemical analysis at Northwest University, Xi'an, China. A portion of the powdered samples was heated at 1000 °C in an oven for 50 minutes to determine Loss on Ignition (LOI.). A further portion of the powdered samples was prepared for X-ray fluorescence (XRF, Rigaku RIX2100) by mixing 0.7 g of sample, 0.3 g LiF, 0.4 g NH_4NO_3, 3.6 g $Li_2B_4O_7$, and 2–3 drops of 1.5% (w/w) LiBr solution. This mixture was melted in a non-wetting precious metal crucible and poured into a glass disk. In addition, 50 mg of sample powder was mixed with $HClO_4$, HNO_3 and HF and digested at 190°C for 48 hours in steel bombs with polytetrafluoroethylene sleeves. After drying, the residues were taken up in 80 mL of 2% HNO_3 with 10 ng/g of Rh as an internal standard. These solutions were analyzed by ICP-MS (Agilent 7500a) for trace elements and REE. The analytical protocol was standardized using international rock standards BCR-2, BHVO-1 and AGV-1. The analytical precision, based on sample replicates, was better than 1% for major oxides and 5–10% for REE and trace elements.

RESULTS

Petrography

Chloritite

Chloritite is a fine-grained and monomineralic rock that shows interlocking or interpenetrating textures. It is composed almost entirely of chlorite (85–95 vol%) with minor talc. The accessory minerals include epidote, rutile, titanite, corundum and opaque minerals. Chlorite occurs as fine dense flaky aggregates (Text-fig. 3a) and locally shows the perfect foliation of the parent rock. It displays pale green, faintly pleochroic and abnormal blue or brown interference colors. Some crystals are pigmented with a reddish brown color due to release of iron oxides. Talc occurs as very fine aggregates with high birefringence. It is formed as an alteration product of chlorite (Text-fig. 3b). Opaque minerals are represented mainly by Fe-Ti oxides, chromite and minor sulphides. Fe-Ti oxides include magnetite, ilmenite, rutile and Fe-oxyhydroxide. Rutile forms fine anhedral or tabular red crystals (Text-fig. 3c). Corundum occurs as aggregates of subhedral to anhedral crystals, while Fe-oxyhydroxide occurs as irregular batches (Text-fig. 3d). Chromite occurs as cracked crystals partly altered to chromian magnetite. Magnetite is present as anhedral to subhedral crystals and is slightly martitized. Epidote occurs as fine aggregates or as veinlets (Text-fig. 3e).

Serpentinite

The serpentinites are massive rocks, but they are sheared at their marginal parts and show subparallel alignment of serpentine flakes resulting in an evident schistosity. The serpentine minerals are the essential components of serpentinite with less amounts of carbonates and opaque minerals. Despite the high degree of serpentinization, rare relicts of olivine (Text-fig. 3f) are present in a few samples. Also, the presence of bastite and mesh textures indicates the former presence of pyroxene and olivine, respectively. Serpentine minerals are mainly represented as antigorite, with lesser amounts of chrysotile and lizardite. Antigorite occurs as flame-like crystals and interpenetrating bladed crystals. A few veins of chrysotile are observed cross-cutting the antigorite matrix. The carbonates include sparse large crystals and fine aggregates of magnesite. The opaque minerals include a few crystals of Cr-spinel, magnetite and sulphides. Cr-spinel occurs as fresh dark brown crystals surrounded by rims of ferritchromite. Magnetite is present as fine-grained disseminated crystals or as straights along the original cleaves planes of pyroxene. Sulphides include a few specks of pyrite and chalcopyrite.

Mineral chemistry

Chlorite

Chlorites were analyzed in chloritite and serpentinite and their chemical compositions and structural formulas are given in the Appendix 1. Chlorite from chloritite contains higher SiO_2 (28.48–31.59 wt.%), FeO (24.28–27.68 wt.%), Cr_2O_3 (0.09–1.67 wt.%),

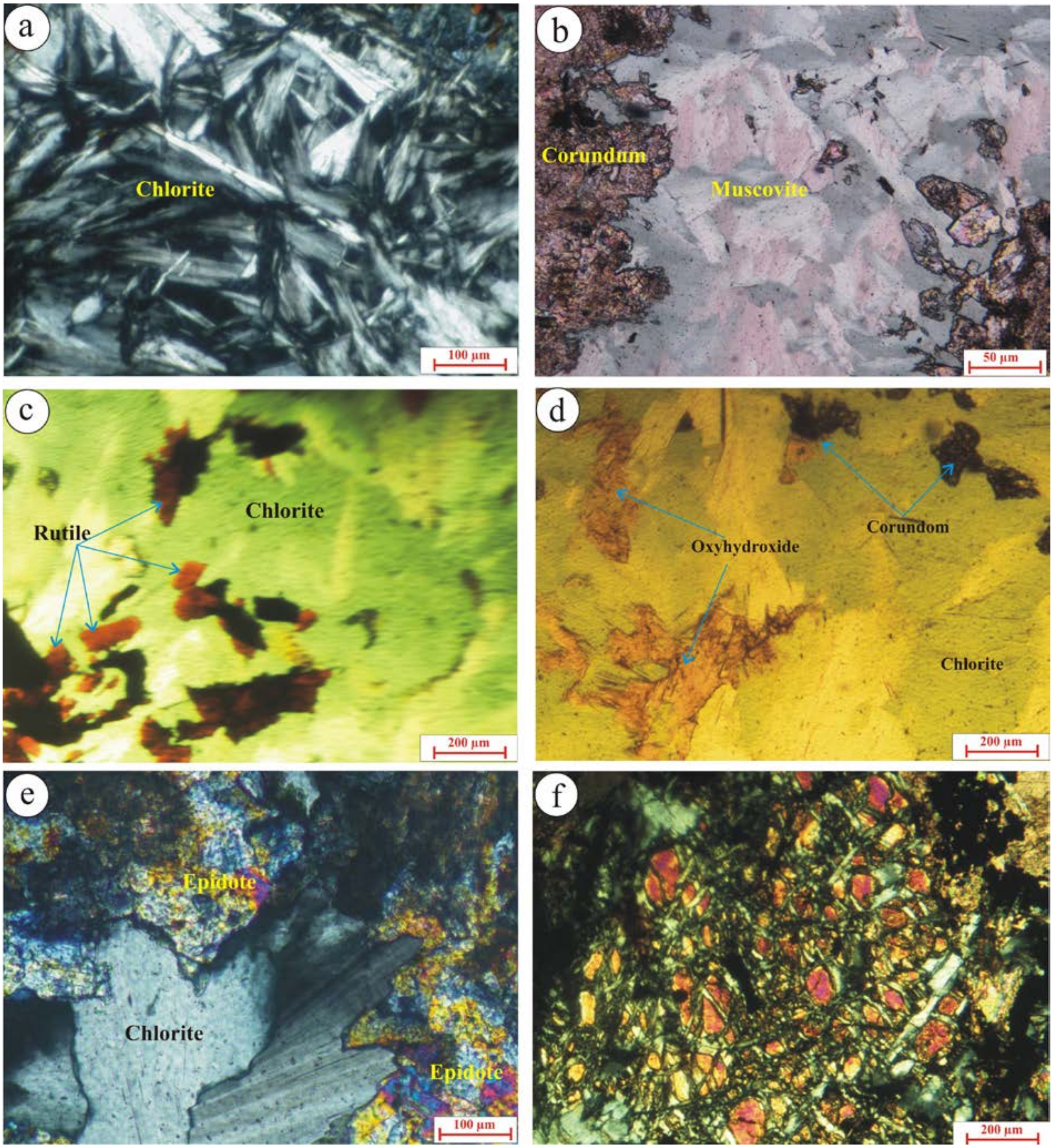

Text-fig. 3. Photomicrographs of chloritite and serpentinite (a, b, e and f are in cross-polarized transmitted light, while c and d are in plane polarized light): (a) flaky aggregates of chlorite, (b) fine aggregates of muscovite and corundum, (c) fine anhedral red crystals of rutile, (d) fine aggregates of corundum and irregular batches Fe-oxyhydroxide, (e) epidote formed after chlorite and (f) fresh relicts of olivine in the serpentinite.

Na_2O (0.03–0.34 wt.%) and K_2O (0.07–1.23 wt.%), but lower Al_2O_3 (13.34–18.39 wt.%) and MgO (9.22–12.28 wt.%) than those from serpentinite (23.66–26.88 wt.% SiO_2, 20.02–22.68 wt.% Al_2O_3, 15.48–16.48 wt.% FeO, 0.02–0.70 wt.% Cr_2O_3, <0.05 wt. % Na_2O, <0.06 wt.% K_2O and 20.08–22.68 wt.% MgO). The TiO_2 and NiO contents are nearly similar in the analyzed chlorites from chloritite and serpentinite. The analyzed chlorite in the chloritite has lower Mg# (0.71–0.47) than those in the serpentinites (Mg# = 0.68–0.72). According to the classification scheme of Hey (1954), chlorite in the chloritite is classified as

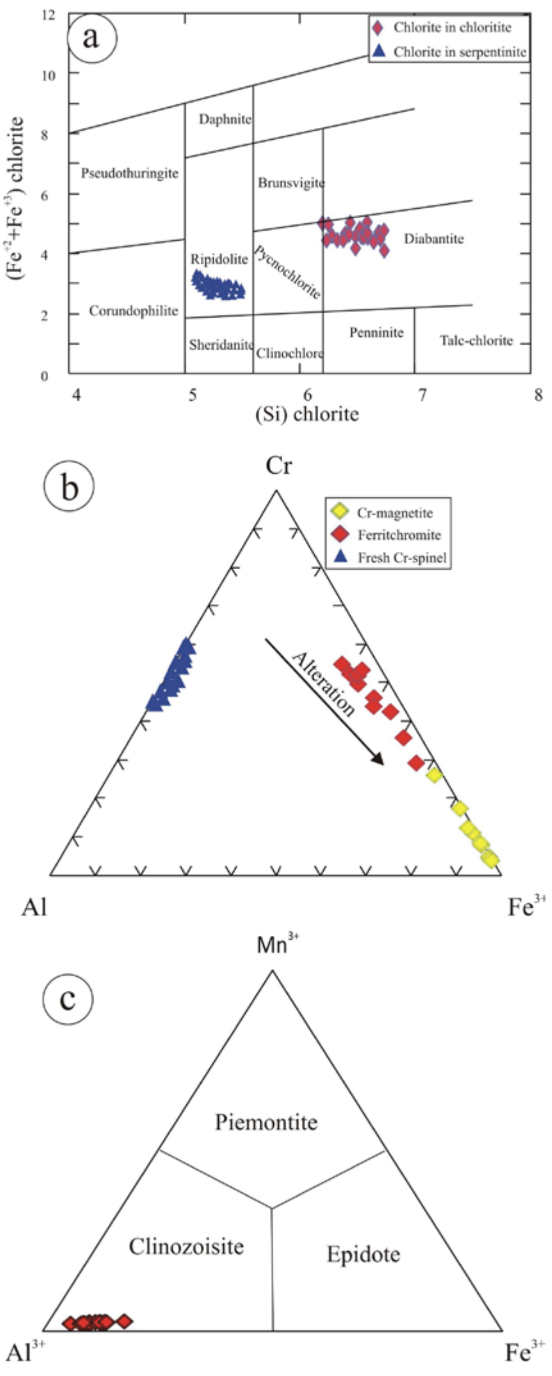

Text-fig. 4. Mineral chemistry diagrams: (a) classification diagram for chlorite-group minerals (Hey 1954), (b) Cr-Al-Fe^{3+} plot of Cr-spinels and their alteration products, and (c) classification of the epidote group (Franz and Liebscher 2004; Armbruster *et al.* 2006).

diabantite, whereas in the serpentinite as ripidolite (Text-fig. 4a).

The chemical composition of chlorite has been used to determine the temperature of its formation by replacement reactions (e.g. Cathelineau and Nieva 1985; Kranidiotis and MacLean 1987; Hillier and Velde 1991; Bourdelle and Cathelineau 2015; Yavuz *et al.* 2015). Calculated temperatures for chlorite formation, on the basis of the Kranidiotis and MacLean (1987) geothermometer, are listed in the Appendix 1. The inferred temperatures for formation of chlorite in chloritite (200–250°C) are lower than those for the serpentinite (310–345°C), suggesting that the chlorite of chloritite may have been formed in a different hydrothermal stage than that responsible of chlorite formation in the serpentinite.

Mica

The analyzed mica in the chloritite is represented by annite; iron end member of the biotite mica group. The chemical analyses of annite and their structural formulae (on the basis of 22 oxygen atoms) are given in Appendix 2. The analyzed annite has TiO_2 between 2.44 and 3.26 wt.% with an average 2.91 wt.%, Al_2O_3 contents between 11.20 and 12.25 wt.% with an average of 11.90 wt.%, FeO between 19.82 and 23.09 wt.% with an average of 21.0 wt.%, MgO between 9.85 and 11.60 wt.% with an average of 10.86 wt.%, K_2O between 7.69 and 9.18 wt.% with an average of 8.76 wt.%. The Mg# ranges between 0.44 and 0.51.

Opaque minerals

The analyzed opaque minerals in the serpentinite include chrome spinel and its alteration products (Appendix 3). The chrome spinel cores are compositionally homogeneous although they exhibit discontinuous opaque rims as a result of their limited alteration to ferritchromite. Chrome spinel cores have 48.33–55.96 wt.% Cr_2O_3, 18.3–23.67 wt.% $FeO_{(t)}$, 12.61–20.2 wt.% Al_2O_3 and 6.42–11.65 wt.% MgO, with negligible amounts of SiO_2, CaO, Na_2O, K_2O, TiO_2, and NiO. Cr# (molar Cr/Cr+Al) of fresh chrome spinel ranges between 0.62 and 0.75 with an average 0.69, whereas Mg# (molar Mg/(Mg+Fe)) displays a wider range (0.33–0.55). The relatively high FeO content in the rims of chrome spinels (52.27–90.06 wt. %) is due to formation of ferritchromite and Cr-magnetite. Development of ferritchromite is a common feature within chromites of ANS ophiolites (e.g., Khalil and Azer 2007; Azer 2014; Khalil *et al.* 2014; Moussa *et al.* 2022). The enrichment in total FeO in ferritchromite and Cr-magnetite is accompanied by depletion in Al_2O_3, Cr_2O_3 and MgO (Text-fig. 4b).

Ferritchromite is richer in MnO (1.92–2.71 wt.%) than fresh chrome spinel (0.43–0.55 wt.%) and Cr-magnetite (0.22–1.01 wt.%)

The analyzed opaque minerals in the chloritite samples are represented by magnetite, Cr-magnetite, ilmenite, ferritchromite and brookite (Appendices 4, 5 and 6). Magnetite and ilmenite are the most abundant Fe-Ti oxides in the chloritite. The magnetite has high FeO (90.48–94.23 wt.%) and low TiO_2 (0.01–0.75 wt.%). The ulvöspinel content in the analyzed magnetite, calculated according to Störmer (1983), is less than 0.02%. Cr-magnetite contains higher Cr_2O_3 (3.05–8.62 wt.%) than the magnetite (0.58–1.07 wt.%).

The analyzed ilmenite is nearly pure end-member ilmenite with TiO_2 content ranging between 49.67 and 52.03 wt.%. According to the procedure of Störmer (1983), the calculated ilmenite contents range between 94 and 99 mol%. Significant substitution of Mn for Fe^{2+} is observed where MnO varies from 3.78 and 12.43wt. %. The essential oxides in the analyzed brookite are TiO_2 (47.92–61.37 wt.%) and FeO (33.61–44.69 wt.%) with minor amounts of MnO (0.14–1.26 wt.%), MgO (0.02–0.18 wt.%) and CaO (0.03–0.29 wt.%). The analyzed ferritchromite of chloritite is rich in MnO (1.68–2.51 wt. %) similar to ferritchromite in the serpentinite.

Epidote

The chemical composition of the analyzed epidote crystals is presented in the Appendix 7. The analyzed epidote crystals show a limited composition range with SiO_2 contents ranging between 37.45 and 38.73 wt.%. They are rich in Al_2O_3 (24.04–27.74 wt.%), FeO (6.5–10.99 wt.%) and CaO (23–24.18 wt.%) with minor amounts of TiO_2 (0.08–0.23 wt.%), MnO (0.14–0.28 wt.%) and MgO (0.01–0.17 wt.%). The analyzed epidote crystals (Text-fig. 4c) correspond to the clinozoisite (Franz and Liebscher 2004; Armbruster *et al.* 2006).

Apatite

The chemical composition and structural formulae of the analyzed apatite crystals are given in the Appendix 8. Apatite analyses have low totals (96.40–98.19 wt.%) because fluorine and chlorine were not analyzed. CaO (54.05–57.44 wt.%) and P_2O_5 (39.66–40.09 wt.%) are the major detected oxides in the apatite, with smaller amounts of FeO (0.06–1.39 wt.%), MnO (0.05–0.18 wt.%) and Na_2O (0.02–0.16 wt.%).

Geochemistry

The bulk rock chemistry data for nine representative samples (6 chloritite and 3 serpentinite) are given in Table 1. Representative serpentinite samples were analyzed for whole rock geochemistry to compare with the associated chloritites. All the serpentinite samples have high LOI values ranging between 13.74% and 14.18% due to extensive serpentinization. The serpentinite samples have SiO_2 content ranging between 36.72 and 38.05 wt.% with enrichment of MgO (37.16–38.03 wt.%) and moderate total iron as Fe_2O_3 (7.08–8.21 wt.%). The analyzed serpentinite samples are depleted in TiO_2 (0.01–0.02 wt.%), Al_2O_3 (0.30–0.38 wt.%), CaO (0.90–1.12 wt.%), MnO (0.13–0.15 wt.%) and P_2O_5 (~0.01 wt.%). The low CaO and Al_2O_3 contents are conformable with the low clinopyroxene abundance and absence of plagioclase. Serpentinite samples have high Mg# [100 molar Mg/(Mg+Fe)] with relatively restricted range (0.90–0.91) comparable with the modern oceanic peridotites (Mg# >0.89, Bonatti and Michael 1989) and the ophiolitic rocks of the ANS (e.g., Azer *et al.* 2013; Ali *et al.* 2020, 2023; Abuamarah 2020; Abuamarah *et al.* 2020; Gahlan *et al.* 2020; Moussa *et al.* 2022). The serpentinites are depleted in most trace elements (Ag, Ba, Be, Bi, Cs, Ga, Hf, Li, Nb, Rb, Sb, Se, Sn, Sr, Ta, Th, W, Y and Zr), except for the enrichment in the compatible trace elements Cr (2720–2869 ppm), Ni (1628–1782 ppm) and Co (116–122 ppm). Also, they are somewhat enriched in some of the compatible elements such as V (32.43–34.24 ppm), Zn (48.40–54.92 wt. %), Cu (5.69–8.86 wt. %) and Sc (4.30–4.80 ppm).

The analyzed chloritite samples contain 11.25–13.31 % LOI, 28.14–31.65 wt.% SiO_2, 0.66–1.76 wt.% TiO_2, 15.08–16.32 Al_2O_3, 29.37–31.10 wt.% MgO, 9.54–13.33 wt.% Fe_2O_3 and 0.24–0.57 wt.% CaO, with traces of other oxides such as Na_2O (0.04–0.11 wt.%), K_2O (0.02–0.05 wt.%) and P_2O_5 (0.03–0.34 wt.%). The chloritite samples contain high concentrations of incompatible high field strength elements such as Zr (27.39–39.34), Hf (0.78–1.24 ppm), Nb (2.47–3.82 ppm) and Ta (0.12–0.17 ppm) and Y (8.94–14.54 ppm) if compared with the serpentinite. They are enriched in the compatible trace elements Cr (2031–2534 ppm), Ni (1264–1988 ppm) and Co (76–101 ppm), similar in this regard to the serpentinite samples.

Primitive mantle (PM)-normalized (McDonough and Sun 1995) trace element patterns for the serpentinite and chloritite samples are presented in Text-fig. 5a. Samples of each rock type show nearly comparable patterns. Serpentinite shows a slight enrichment in the large ion lithophile elements (LILE)

	Rock type	Chloritite						Serpentinite		
	Sample No.	**CHL-1**	**Um17**	**Br19**	**Br53**	**CHL-5**	**Br56**	**SRP-1**	**SRP-2**	**SRP-3**
Major oxides (wt. %)	SiO_2	29.19	29.13	29.8	28.14	31.65	30.07	37.3	36.72	38.05
	TiO_2	0.66	0.74	0.88	1.58	0.85	1.76	0.01	0.02	0.01
	Al_2O_3	16.13	15.82	16.3	15.08	16.32	15.45	0.34	0.38	0.3
	Fe_2O_3	10.43	10.58	9.54	12.38	12.05	13.33	7.97	8.21	7.08
	MnO	0.11	0.08	0.07	0.14	0.13	0.14	0.13	0.14	0.15
	MgO	30.70	30.42	31.1	29.7	30.17	29.37	37.16	37.84	38.03
	CaO	0.31	0.24	0.43	0.31	0.35	0.57	1.03	0.9	1.12
	Na_2O	0.04	0.11	0.05	0.04	0.05	0.06	<dl	<dl	<dl
	K_2O	0.04	0.02	0.03	0.02	0.04	0.05	<dl	<dl	<dl
	P_2O5	0.02	0.03	0.02	0.16	0.28	0.34	0.01	0.01	0.01
	LOI	11.42	12.48	12.15	11.25	13.31	12.11	13.74	14.08	14.18
	Total	99.06	99.65	99.81	98.81	99.19	99.35	98.37	99.33	98.9
Trace elements (ppm)	Sc	36.75	31.18	29.44	32.24	34.67	31.14	4.45	4.8	4.3
	Ba	16.29	19.14	33	18.21	22.11	24.89	2.79	3.54	4.91
	Be	0.27	0.24	0.19	0.31	0.11	0.13	0.07	0.09	0.05
	Ni	1855.98	1988.15	1554.41	1263.91	1397.65	1289.12	1781.7	1627.5	1667.78
	Co	93.95	89.79	76.1	94.05	101.11	98.94	116.26	122.31	119.51
	Cr	2533.87	2347.04	2235.87	2030.64	2255.38	2234.56	2719.62	2869.37	2763.31
	Cs	0.03	0.02	0.04	0.06	0.03	0.05	0.01	<dl	0.01
	Ga	12.11	11.74	13.15	10.61	11.08	12.76	0.56	0.67	0.48
	Hf	0.87	1.01	0.78	1.24	0.89	1.11	0.02	0.03	0.01
	Nb	3.37	2.56	3.74	3.82	3.44	2.47	0.46	0.61	0.35
	Rb	2.01	1.94	1.49	2.21	1.94	2.17	0.34	0.61	0.49
	Sn	0.61	0.53	0.48	0.86	0.54	0.61	2.52	1.77	0.95
	Sr	16.30	14.45	12.35	18.78	20.45	29.87	3.64	5.92	4.4
	Ta	0.15	0.13	0.14	0.12	0.17	0.15	0.01	0.02	0.01
	Th	0.28	0.26	0.24	0.31	0.29	0.27	0.03	0.04	0.05
	U	0.11	0.09	0.13	0.08	0.15	0.12	0.01	0.02	0.01
	V	87.37	97.34	84.16	90.11	62.59	71.45	32.43	34.24	32.65
	W	0.87	0.78	0.96	0.89	1.27	1.35	0.34	0.25	0.41
	Zr	27.39	27.87	31.77	39.34	33.22	35.16	1.01	0.92	0.84
	Y	8.94	10.82	11.09	10.76	14.54	13.24	0.37	0.41	0.35
	Mo	0.56	0.74	0.48	0.37	0.44	0.51	0.17	0.22	0.31
	Cu	1.96	2.04	1.77	1.14	3.22	4.6	5.69	8.86	7.1
	Pb	9.43	11.47	6.1	6.74	5.32	4.74	0.19	0.23	0.31
	Zn	79.40	74.39	71.9	62.39	84.14	101.08	50.19	48.4	54.92
	As	0.37	0.44	0.42	0.66	0.64	0.43	1.98	2.14	1.56
	Sb	0.26	0.24	0.24	0.35	0.27	0.31	0.56	0.42	0.33
	Bi	0.06	0.05	0.05	0.07	0.06	0.07	0.05	0.03	0.04
REE (ppm)	La	1.489	1.711	1.522	1.317	2.024	1.835	0.086	0.093	0.077
	Ce	4.647	5.197	4.455	4.152	6.485	5.525	0.213	0.233	0.183
	Pr	0.758	0.872	0.735	0.693	1.093	0.915	0.031	0.035	0.028
	Nd	3.945	4.553	3.645	3.483	5.644	4.755	0.148	0.166	0.132
	Sm	1.241	1.458	1.207	1.173	1.805	1.552	0.045	0.051	0.042
	Eu	0.212	0.243	0.255	0.201	0.335	0.265	0.016	0.018	0.014
	Gd	1.563	1.713	1.881	1.588	2.385	2.103	0.059	0.064	0.054
	Tb	0.304	0.326	0.335	0.307	0.438	0.394	0.01	0.011	0.009
	Dy	2.060	2.154	2.253	2.057	2.774	2.481	0.063	0.075	0.058
	Ho	0.419	0.449	0.471	0.418	0.604	0.552	0.014	0.016	0.012
	Er	1.122	1.225	1.285	1.106	1.668	1.434	0.039	0.047	0.034
	Tm	0.166	0.182	0.193	0.164	0.25	0.229	0.006	0.007	0.005
	Yb	1.048	1.151	1.215	1.033	1.537	1.366	0.039	0.048	0.033
	Lu	0.166	0.184	0.194	0.164	0.247	0.219	0.006	0.007	0.005
	Eu/Eu*	0.47	0.47	0.52	0.45	0.49	0.45	0.95	0.96	0.90
	(La/Yb)n	0.96	1.01	0.85	0.86	0.89	0.91	1.49	1.31	1.58
	(La/Sm)n	0.76	0.74	0.80	0.71	0.71	0.75	1.21	1.15	1.16
	(Gd/Lu)n	1.15	1.14	1.19	1.19	1.18	1.18	1.21	1.12	1.32
	(La/Lu)n	0.92	0.95	0.80	0.82	0.84	0.86	1.47	1.36	1.58

Table 1. Whole rock chemical analyses of chloritite and associated serpentinites of Al-Barramiya ophiolite

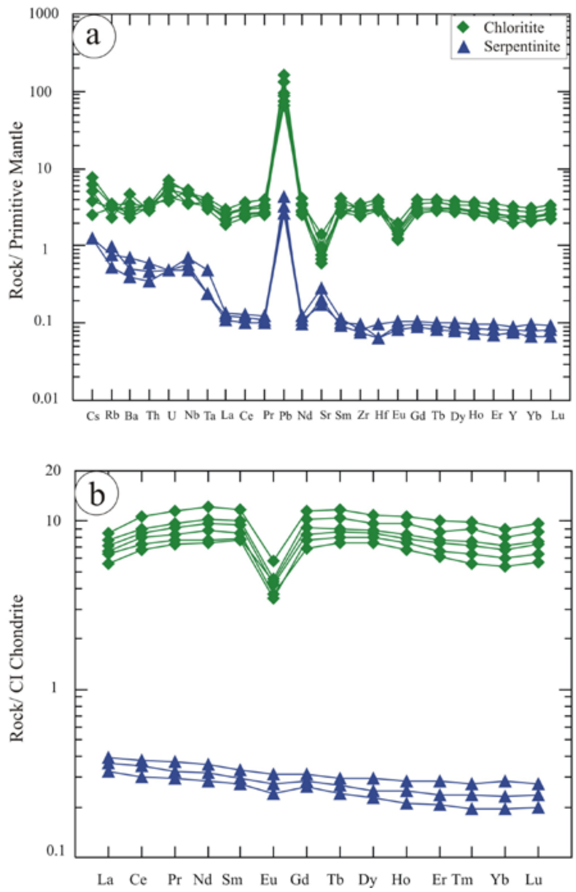

Text-fig. 5. Whole-rock geochemistry of the chloritite: (a) Primitive mantle-normalized trace element patterns for the chloritite and serpentinite, and (b) Chondrite-normalized rare earth element patterns for chloritite and serpentinite; normalization values for (a) and (b) are from McDonough and Sun (1995).

compared with the high-field strength elements (HFSE) with positive anomaly in Pb. Also, chloritites show a positive anomaly in Pb, but negative anomalies in Sr and Eu.

Chondrite-normalized (McDonough and Sun 1995) REE patterns for serpentinite and chloritite samples are presented in Text-fig. 5b. Serpentinite samples are much depleted in REE (0.70–0.87 ppm) than the chloritite samples (17.86–27.29 ppm). The analyzed serpentinite samples show nearly similar REE patterns and are depleted relative to CI-chondrite values. They are characterized by slight enrichment in light rare earth elements (LREE) relative to heavy rare earth elements (HREE) [(La/Lu)n = 1.36–1.58] with slightly negative Eu-anomaly [(Eu/Eu*)n = 0.90–0.96].

The chloritite samples show similar REE patterns, but are enriched relative to CI-chondrite values. They are characterized by their being slightly depleted in LREE relative to HREE [(La/Lu)n = [0.80–0.95].The lower LREE concentrations are presumably related to the monomineralic (chlorite) characteristic of this rock type. REE patterns of chloritite samples have moderately negative Eu-anomaly [(Eu/Eu*)n = 0.45–0.52], despite their neither containing nor having interacted with plagioclase. The negative Eu-anomaly may be likely derived from chloritization fluids or it might reflect the occasional presence of talc in the chloritite, which excludes Eu relative to neighboring REE (Cárdenas-Párraga *et al.* 2017).

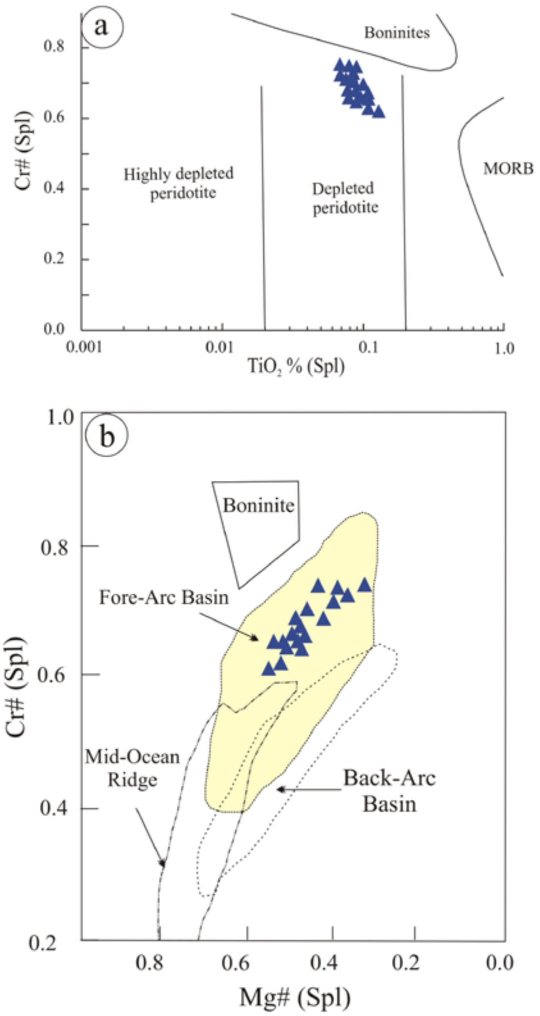

Text-fig. 6. Tectonic discrimination diagrams for serpentinite based mineral chemistry. (a) Cr# vs. TiO_2 diagram for the fresh Cr-spinels. The fields are according to Dick and Bullen (1984); Jan and Windley (1990); Arai (1992). (b) Cr# vs. Mg# diagram for fresh Cr-spinels (after Stern *et al.* 2004); the field boundaries are from Dick and Bullen (1984), Bloomer *et al.* (1995) and Ohara *et al.* (2002).

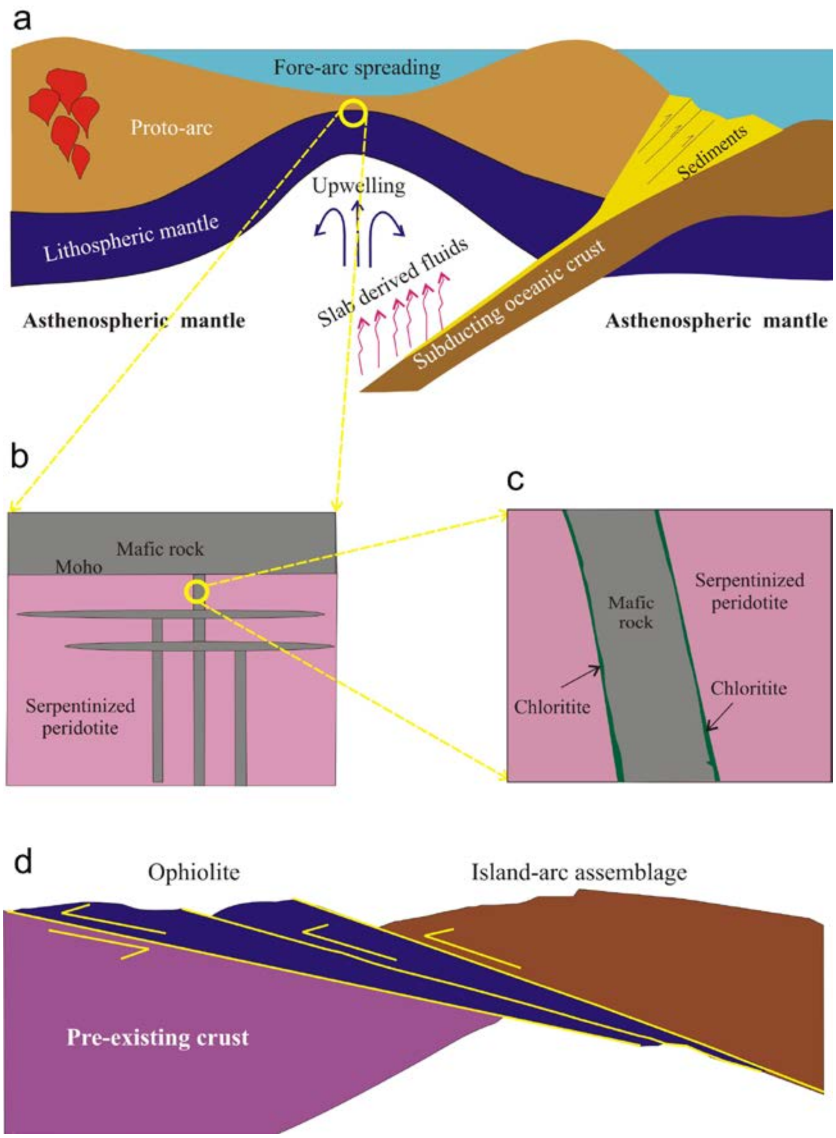

Text-fig. 7. The sequence of events for formation of Al-Barramiya ophiolite: (a) fore-arc spreading and formation of ophiolitic mantle section, (b) emplacement of mafic rocks, (c) serpentinization and chloritization processes, and (d) obduction of the ophiolite sequence causing brittle shear deformation.

PETROGENESIS

Different tectonic settings have been proposed for the evolution of Egyptian ophiolites including mid-ocean ridge (MOR) and supra-subduction zone (SSZ) environments (Zimmer *et al.* 1995; Stern *et al.* 2004; Azer and Stern 2007). Nowadays, the SSZ, especially as a fore-arc environment, is the more acceptable tectonic setting for the Egyptian ophiolites (El Sayed *et al.* 1999; Ahmed *et al.* 2001; Farahat *et al.* 2004; Azer and Khalil 2005). Other studies prefer a back-arc position to explain the origin of these ophiolites (Azer and Stern 2007; Abd El-Rahman *et al.* 2009; Azer 2014; Khalil *et al.* 2014; Gahlan *et al.* 2015, 2018; Obeid *et al.* 2016; Azer *et al.* 2019, Moussa *et al.* 2021, 2022).

The presence of bastite and mesh textures together with high Cr, Ni and Co in the serpentinites associated with chloritite indicate a depleted, dunite-harzburgite protolith. The low MgO/SiO_2 ratios (1.00–1.03) and low TiO_2 contents (0.01–0.02 wt.%) of the serpentinite is comparable with supra-subduction zone depleted peridotites, especially from fore-arc setting (e.g., Deschamps *et al.* 2013; Salters and Stracke 2004).

Also, their very low Al_2O_3 (0.30–0.38 wt.%) and CaO (0.90–1.12 wt.%) resemble those of fore-arc peridotites (e.g. Ishii *et al.* 1992). This is supported by very low Al_2O_3/SiO_2 ratios ~ 0.01, which is thought to suggest a forearc setting, since the serpentinization process should have a negligible influence on the Al_2O_3/SiO_2 ratio (e.g. Paulick *et al.* 2006; Deschamps *et al.* 2013), if quartz veins are avoided.

Chrome spinel represents a sensitive petrogenetic indicator (e.g. Dick and Bullen 1984; Barnes and Roeder 2001; Ohara *et al.* 2002; Sobolev and Logvinova 2005; Arif and Jan 2006; Uysal *et al.* 2012). On the Cr# vs. TiO_2 diagram (Text-fig. 6a), the analyzed fresh chrome spinel plots in the field of depleted mantle. The low TiO_2 (0.07–0.13 wt.%) and high Cr# (0.62–0.75) of the chrome spinel indicate that they are residuals from high-degree partial melting (e.g. Uysal *et al.* 2012) and similar to those of modern fore-arc peridotites (Text-fig. 6b).

The published papers about the origin of chloritite rocks are limited in number over the world (David *et al.* 1990; Ramos *et al.* 2018; Compagnoni *et al.* 2021). According to Barnes and O'Neil (1969), chloritization of the ultramafics is characterized by an increase in TiO_2, Al_2O_3 and FeO and a decrease in SiO_2 and CaO contents and can probably be ascribed to the effect of the nearby granitic intrusion. Deer et al. (1992) reported that the formation of chlorite is mostly at a temperature less than 400˚C.

Some previous studies have focused on the chloritite rocks in the Eastern Desert of Egypt, but their origin is still controversial and debated. Some researchers believed that these chlorites are related to ultramafic rocks (Basta and Kader 1969; Abdel Kader 1974; Takla and Noweir 1980; Takla *et al.* 1991, 1992, 2003), while others considered them as being a part of paraschists, belonging to geosynclinal metasediments (El-Ramly and Akaad 1960; Akaad and Noweir 1980). Takla et al. (1991) considered that the chlorites are the products of retrograde metamorphism simultaneously with the obduction and thrusting of the ophiolitic ultramafics. During the chloritization of serpentinites Ca, Fe and Si were released while Al and Mg were precipitated from the Mg-Al rich solutions to form Mg-Al (Fe) chloritite. This is consistent with the chemical analyses of the chlorite in the studied chloritite which shows enrichment of Mg, Al and Fe.

In the present study, the occurrence of chloritite as layers around the serpentinized ultramafics suggests a direct relationship with them. The high contents of Cr (2031–2534 ppm), Co (76–101 ppm) and Ni (1264–1988 ppm) of the studied chloritite samples are close to those of the associated serpentinites (Cr = 2720–2869 ppm, Ni = 1628–1782 ppm, Co = 116–122 ppm), supporting their relation with the ophiolitic ultramafic rocks. Therefore, we interpret the studied chloritite as derived by the metasomatic alteration of nearby ultramafic rocks.

The sequence of events for the formation of the Al-Barramiya ophiolite including serpentinization and chloritization processes and the subsequent obduction of the ophiolite sequence causing brittle shear deformation is represented schematically in Text-fig. 7. This model shows the formation of the Al-Barramiya ophiolite in a fore-arc spreading center with emplacement of sills and dikes of mafic rocks into harzburgite near the crust-mantle transition in the fore-arc oceanic lithosphere. Then, the whole ophiolitic sequence obducted over the old continental crust.

CONCLUSION

- Chloritite in the Al-Barramiya area occurs as thin rims around the peripheries of serpentinized peridotite. It is fine-grained and consists in the majority of chlorite (85–95 %) with minor talc. Epidote, rutile, titanite, corundum and opaque minerals are the accessory minerals.
- Chloritite samples are characterized by their being slightly depleted in LREE relative to HREE [(La/Lu)n = 0.80–0.95] with moderately negative Eu-anomaly [(Eu/Eu*)n = 0.45–0.52]. The negative Eu-anomalies are derived from chloritization fluids or reflect the presence of talc in the chloritite.
- The chlorite of the chloritite formed at temperatures ranging between 200 and 250 °C which is lower than the temperature for the disseminated chlorite in the serpentinite (310–345°C), indicating its formation in a different hydrothermal stage.
- The Al-Barramiya chloritite was formed as a secondary product which was derived from associated serpentinized ultramafics via hydrothermal alterations. This is supported by the high contents of Cr (2031–2534 ppm), Ni (1264–1988 ppm) and Co (76–101 ppm) in the analyzed chloritite samples comparable to that of the host serpentinite (2720–2869 ppm Cr, 1628–1782 ppm Ni and 116–122 ppm Co).
- The geochemical characteristics of the Al-Barramiya serpentinite, the host of chloritite, are substantially similar to those formed in a fore arc setting within a supra-subduction zone environment.

Acknowledgement

This work was supported by King Saud University (Researchers Supporting Project number RSP2024R151), which covered all analytical costs in Canada and China. The efforts given by the Editor (Prof. Piotr Łuczyński) and the three reviewers (Prof. Avishai Abbo, Prof. Grzegorz Gil and anonymous) are highly appreciated. Also, this article is partly supported by the Academy of Scientific Research and Technology under the fellowship program "Short Term Research & Technology Transfer (ASRT-STARS).

REFERENCES

Abd El-Rahman, Y., Polat, A., Dilek, Y., Fryer, B.J., El-Sharkawy, M. and Sakran, S. 2009. Geochemistry and tectonic evolution of the Neoproterozoic incipient arc-fore-arc crust in the Fawakhir area, Central Eastern Desert of Egypt. *Precambrian Research*, **175**, 116–134.

Abdel Kader, Z. 1974. Mineralogical and geochemical studies on some Egyptian Mg-rich layer silicates (chloritites, serpentinites and talcs), 270 pp. PhD thesis, Cairo University.

Abdel-Karim, A.M. 2000. Chlorite schists and rodingites in the mafic-ultramafic rocks from the central Eastern Desert of Egypt: Petrogenesis and metamorphic history. *Earth Science Series*, **14**, 150–170.

Abuamarah, B.A. 2020. Geochemistry and fore-arc evolution of upper mantle peridotites in the Cryogenian Bir Umq ophiolite, Arabian Shield, Saudi Arabia. *International Geology Review*, **62**, 630–648.

Abuamarah, B.A., Alshehri, F., Azer, M.K. and Asimow, P.D. 2023. Geological and tectonic significance of rodingite in the Ess ophiolite, Arabian Shield, Saudi Arabia. *Lithos*, **448**, p.107168.

Abuamarah, B.A., Asimow, P.D., Azer, M.K. and Ghrefat, H. 2020. Suprasubduction-zone origin of the podiform chromitites of the Bir Tuluhah ophiolite, Saudi Arabia, during Neoproterozoic assembly of the Arabian Shield. *Lithos*, **360–361**, 105439.

Ahmed, A.H., Arai, S. and Attia, A.K. 2001. Petrological characteristics of podiform chromitites and associated peridotites of the Pan African ophiolite complexes of Egypt. *Mineralium Deposita*, **36**, 72–84.

Akaad, M.K. and Noweir, M.A. 1980. Geology and lithostratigraphy of the Arabian Desert orogenic belt of Egypt between latitudes 25° 35′ and 26° 30′ N. *Bulletin of Institute of Applied Geology, King Abdul Aziz University Jeddah*, **4**, 127−134.

Ali, R.A.M., Pitcairn, I.K., Maurice, A.E., Azer, M.K., Bakhit, B.R. and Shahien, M.G. 2020. Petrology and geochemistry of ophiolitic ultramafic rocks and chromitites across the Eastern Desert of Egypt: Insights into the composition and nature of a Neoproterozoic mantle and implication for the evolution of SSZ system. *Precambrian Research*, **337**, 105565.

Ali, S., Azer, M. and Abdel-Karim, A.A. 2023. Origin and evolution of Neoproterozoic metaophiolitic mantle rocks from the eastern Desert of Egypt: Implications for tectonic and metamorphic events in the Arabian-Nubian Shield. *Geologica Acta*, **21** (6), 1–21, I–VII.

Arai, S. 1992. Chemistry of chromian spinel in volcanic rocks as a potential guide to magma chemistry. *Mineralogical magazine*, **56**, 173–184.

Arif, M., Jan, M.Q. 2006. Petrotectonic significance of the chemistry of chromite in the ultramafic-mafic complexes of Pakistan. *Journal of Asian Earth Sciences*, **27**, 628–646.

Armbruster, T., Bonazzi, P., Akasaka, M., Bermanec, V., Chopin, C., Gieré, R., Heuss-Assbichler, S., Liebscher, A., Menchetti, S., Pan, Y. and Pasero, M. 2006. Recommended nomenclature of epidote-group minerals. *European Journal of Mineralogy*, **18** (5), 551–567.

Azer, M.K. 2014. Petrological studies of Neoproterozoic serpentinized ultramafics of the Nubian Shield: Spinel compositions as evidence of the tectonic evolution of the Egyptian ophiolites.*Acta Geologica Polonica*, **64**, 113–127.

Azer, M.K., Gahlan, H.A., Asimow, P.D., Mubarak, H.S. and Al-Kahtany, K.M. 2019. Multiple stages of carbonation and element redistribution during formation of ultramafic-hosted magnesite in Neoproterozoic ophiolites of the Arabian-Nubian Shield, Egypt. *Journal of Geology*, **127** (1), 81–107.

Azer, M.K. and Khalil, A.E.S. 2005. Petrological and mineralogical studies of Pan-African serpentinites at Bir Al-Edeid area. Central Eastern Desert, Egypt. *Journal of African Earth Sciences*, **43**, 525–536.

Azer, M.K., Samuel, M.D., Ali, K.A., Gahlan, H.A., Stern, R.J., Ren, M. and Moussa, H.E. 2013. Neoproterozoic ophiolitic peridotites along the Allaqi-Heiani Suture, South Eastern Desert, Egypt. *Mineralogy and Petrology*, **107**, 829–848.

Azer, M.K. and Stern, R.J. 2007. Neoproterozoic (835–720 Ma) serpentinites in the Eastern Desert, Egypt: Fragments of fore-arc mantle. *The Journal of Geology*, **115**, 457–472.

Barnes, I. and O'Neil, J.R. 1969. The relationship between fluids in some fresh alpine-type ultramafics and possible modern serpentinization, western United States. *Geological Society of America Bulletin*, **80**, 1947–1960.

Barnes, S.J. and Roeder, P.L. 2001. The Range of Spinel Compositions in Terrestrial Mafic and Ultramafic Rocks. *Journal of Petrology*, **42**, 2279–2302.

Basta, E.Z. and Kader, Z.A. 1969. The mineralogy of Egyptian serpentinites and talc-earbonates. *Mineralogical Magazine,* **37**, 394–408.

Bloomer, S.H., Taylor, B., MacLeod, C.J., Stern, R.J., Fryer, P., Hawkins, J.W. and Johnson, L. 1995. Early arc volcanism and ophiolite problem: A perspective from drilling in the Western Pacific. In: Taylor, B. and Natland, J. (Eds), Active

Margins and Marginal Basins of the Western Pacific, Geophysical Monograph, Vol. 88, 1–30. American Geophysical Union; Washington, DC.

Bonatti, E. and Michael, P.J. 1989. Mantle peridotites from continental rifts to oceanic basins to subduction zones. *Earth and Planetary Science Letters*, **91**, 297–311.

Bourdelle, F. and Cathelineau, M. 2015. Low-temperature chlorite geothermometry: a graphical representation based on a T–R^{2+}–Si diagram. *European Journal of Mineralogy*, **27**, 617–626.

Cárdenas-Párraga, J., García-Casco, A., Proenza, J., Harlow, G., Blanco-Quintero, I., Lázaro, C., Villanova-de-Benavent, C. and Núñez Cambra, K. 2017. Trace-element geochemistry of transform-fault serpentinite in high-pressure subduction mélanges (eastern Cuba): Implications for subduction initiation. *International Geology Review*, **59**, 2041–2064.

Cathelineau, M. and Nieva, D. 1985. A chlorite solid solution geothermometer. The Los Azufrez (Mexico) geothermal system. *Contributions to Mineralogy and Petrology*, **91**, 235–244.

Compagnoni, R., Cossio, R. and Regis, D. 2021. Corundum-bearing veins in chloritite from the Etirol-Levaz Austroalpine continental Slice (Val Tournenche, Aosta, Italy). *Ofioliti*, **46** (2), 119–129.

David, H., Tegyey, M., Le Metour, J. and Wyns, R. 1990. Chloritite vessels from the sultanate of Oman: a petrographical study applied to archeology, 951–958. Academy of Sciences; Paris.

Deer, W.A., Howie, R.A. and Zussman, J. 1992. An introduction to the rock-forming minerals, 698 pp. Longman Group Ltd; New York.

Deschamps, F., Godard, M., Guillot, S. and Hattori, K. 2013. Geochemistry of subduction zone serpentinites: A review. *Lithos*, **178**, 96–127.

Dick, H.J.B. and Bullen, T. 1984. Chromian spinel as a petrogenetic indicator in abyssal and Alpine-type peridotites and spatially associated lavas. *Contribution to Mineralogy and Petrology*, **86**, 54–76.

El Sayed, M.M., Furnes, H. and Mohamed, F.H. 1999. Geochemical constraints on the tectonomagmatic evolution of the late Precambrian Fawakhir ophiolite, Central eastern Desert, Egypt. *Journal of African Earth Sciences*, **29**, 515–533.

El-Ramly, M.F. and Akaad, M.K. 1960. The basement complex in the Central Eastern Desert of Egypt between lat. 24°30 and 25°40 N. *Geological Survey of Egypt, Paper*, **35** (8), 1–32.

Farahat, E.S., El Mahalawi, M.M. and Hoinkes, G. 2004. Continental back-arc basin origin of some ophiolites from the Eastern Desert of Egypt. *Mineralogy and Petrology*, **82**, 81–104.

Franz, G. and Liebscher, A. 2004. Physical and chemical properties of the epidote minerals – an introduction. *Reviews in Mineralogy and Geochemistry*, **56** (1), 1–81.

Gahlan H., Arai S. and Almadani, S.2015. Petrogenesis of carbonated meta-ultramafic lenses from the Neoproterozoic Heiani ophiolite, South Eastern Desert, Egypt: A natural analogue to CO_2 sequestration. *Journal of African Earth Sciences*, **102**, 102–115.

Gahlan, H.A., Azer, M.K. and Al-Kahtany, K.M. 2021. Petrogenesis and geodynamic setting of high-Cr chromitites in fore-arc peridotites: A case study from the Halaban ophiolite, Eastern Arabian Shield, Saudi Arabia. *Lithos*, **396**, 106243.

Gahlan, H.A., Azer, M.K. and Asimow, P.D. 2018. On the relative timing of listvenite formation and chromian spinel equilibration in serpentinites. *American Mineralogist*, **103** (7), 1087–1102.

Gahlan, H.A., Azer, M.K., Asimow, P.D., Mubarak, H.S. and Al-Kahtany, K.M. 2020. Petrological characteristics of the Neoproterozoic Ess ophiolite mantle section, Arabian Shield, Saudi Arabia: a mineral chemistry perspective. *International Journal of Earth Sciences*, **109**, 239–251.

Hey, M.H. 1954. A new review of the chlorites. *Mineralogical Magazine*, **30**, 272–292.

Hillier, S. and Velde, B. 1991. Octahedral occupancy and the chemical composition of diagenetic (low-temperature) chlorites. *Clay Minerals*, **26**, 149–168.

Ishii, T., Robinson, P.T., Maekawa, H. and Fiske, R. 1992. Petrological studies of peridotites from diapiric Serpentinite Seamounts in the Izu-Ogasawara-Mariana forearc, leg 125. In: Pearce, J., Stokking, L.B., *et al.* (Eds), Proceedings of the Ocean Drilling Project, Leg 125, 445–485. Scientific Results (College Station); Texas.

Jan, M.Q. and Windley, B.F. 1990. Chromian spinel-silicate chemistry in ultramafic rocks of the Jijal complex, northwest Pakistan. *Journal of Petrology*, **31**, 667–715.

Khalil, A.E.S. and Azer, M.K. 2007. Supra-subduction affinity in the Neoproterozoic serpentinites in the Eastern Desert, Egypt: evidence from mineral composition. *Journal of African Earth Sciences*, **49**, 136–152.

Khalil, A.E.S., Obeid, M.A. and Azer, M.K. 2014. Serpentinized Peridotites at the North Part of the Wadi Allaqi District (Egypt): Implications for the Tectono-Magmatic Evolution of Fore-arc Crust. *Acta Geologica Sinica-English Edition*, **88** (5), 1421–1436.

Kotschoubey, B., Villas, R.N. and Aires, B. 2016. Chloritites of the Tocantins Group, Araguaia fold belt, central-northern Brazil: Vestiges of basaltic magmatism and metallogenetic implications. *Journal of South American Earth Sciences,* **69**, 171–193.

Kranidiotis, P. and MacLean, W.H. 1987. The systematics of chlorite alteration at the Phelps Dodge massive sulfide deposit, Matagami, Quebec. *Economic Geology*, **82**, 1898–1911.

McDonough, W.F. and Sun, S.S. 1995. Composition of the Earth. *Chemical Geology*, **120**, 223–253.

Moussa, H.E., Azer, M.K., Abou El Maaty, M.A., Maurice, A.E., Yanni, N.N., Akarish, A.I., Elnazer, A.A. and Elsagheer, M.A. 2021. Carbonation of Neoproterozoic mantle section and formation of gold-bearing listvenite in the Northern Nubian Shield. *Lithos*, **406**–**407**, 106525.

Moussa, H.E., Mubarak, H.S., Azer, M.K., Surour, A.A., Asimow, P.D. and Kabesh, M.M. 2022. Multistage petrogenetic evolution of Neoproterozoic serpentinized ultramafic rocks and podiform chromitites at Hagar Dungash, Eastern Desert of Egypt. *Precambrian Research*, **369**, 106507.

Mubarak, H.S., Azer, M.K., Surour, A.A., Moussa, H.E., Asimow, P.D. and Kabesh, M.M. 2020. Mineralogical and geochemical study of rodingites and associated serpentinized peridotite, Eastern Desert of Egypt, Arabian-Nubian Shield. *Lithos*, **374**, 105720.

Obeid, M.A., Khalil, A.E.S. and Azer, M.K. 2016. Mineralogy, geochemistry and geotectonic significance of the Neoproterozoic ophiolite of Wadi Arais area, south Eastern Desert, Egypt. *Internal Geological Review*, **58**, 687–702.

Ohara, Y., Stern, R.J., Ishii, T., Yurimoto, H. and Yamazaki, T. 2002. Peridotites from the Mariana Trough: first look at the mantle beneath an active back-arc basin. *Contribution to Mineralogy and Petrology*, **143**, 1–18.

Paulick, H., Bach, W., Godard, M., Hoog, C.J., Suhr, G. and Harvey, J. 2006. Geochemistry of abyssal peridotites (Mid-Atlantic Ridge, 15 20′N, ODP Leg 209): implications for fluid/rock interaction in slow spreading environments. *Chemical Geology*, **234**, 179–210.

Ramos, R.C., Koester, E., Vieira, D.T., Porcher, C.C., Gezatt, J.N., Fontes, T.P. and Silveira, R.L. 2018. A hybrid origin for the chloritite of the Arroio Grande Ophiolite (Southernmost Brazil) from U-Pb shrimp ages. In: Proceedings of the 49. Brazilian Congress of Geology; 7. Symposium on volcanism and associated environments; 9. Symposium of cretaceous from Brazil, 1–5, Federal University of Rio Grande do Sul, Brasil.

Salters, V.J.M. and Stracke, A. 2004 Composition of the depleted mantle. *Geochemistry, Geophysics, Geosystems*, **5** (5), Q05B07.

Shackleton, R.M. 1994. Review of late Proterozoic sutures, ophiolitic mélanges and tectonics of eastern Egypt and north Sudan. *Geological Rundschau*, **83**, 537–546.

Sobolev, N.V. and Logvinova, A.M. 2005. Significance of accessory chrome spinels in identifying serpentinite paragenesis. *International Geological Review*, **47**, 58–64.

Stern, R.J. 1994. Arc assembly and continental collision in the Neoproterozoic East African Orogen: implications for the consolidation of Gondwanaland. *Annual Reviews of Earth and Planetary Science*, **22**, 319–351.

Stern, R.J., Johnson, P.R., Kröner, A. and Yibas, B. 2004. Neoproterozoic ophiolites of the Arabian-Nubian Shield. In: Kusky, T.M. (Ed.), Precambrian ophiolites and related rocks. *Developments in Precambrian Geology*, **13**, 95–128.

Stormer, J.C. 1983. The effects of recalculation on estimates of temperature and oxygen fugacity from analyses of multicomponent iron-titanium oxides. *American Mineralogist*, **68** (5–6), 586–594.

Takla, M.A., Basta, F.F. and Surour, A.A. 1991. Chloritites at the contacts of some ophiolitic ultramafics, Eastern Desert, Egypt. *Egyptian Mineralogist*, **3**, 151–165.

Takla, M.A., Basta, F.F. and Surour, A.A. 1992. Petrology and Mineral Chemistry of Rodingites associating the Pan-African Ultramafics of Sikait-Abu Rusheid area, South Eastern Desert, Egypt. *Geology of the Arab World*, **1**, 491–507.

Takla, M.A. and Noweir, M.A. 1980. Mineralogy and mineral chemistry of the ultramafic mass of El-Rubshi Eastern Desert, Egypt. *Neues Jahrbuch für Mineralogie-Abhandlungen*, **140**, 17–28.

Takla, M.A., Trommsdorff, V., Basta, F.F. and Surour, A.A. 2003. Margarite in ultramafic alteration zones (Blackwall) A new occurrence in Barramiya Area, Egypt. *European Journal of Mineralogy*, **15** (6), 991–999.

Uysal, I., Ersoy, E.Y., Karslı, O., Dilek, Y., Sadıklar, M.B., Ottley, C.J., Tiepolo, M. and Meisel, T. 2012. Coexistence of abyssal and ultra-depleted SSZ type mantle peridotites in a Neo-Tethyan Ophiolite in SW Turkey: Constraints from mineral composition, whole-rock geochemistry (major-trace-REE-PGE), and Re Os isotope systematic. *Lithos*, **132**–**133**, 50–69.

Yavuz, F., Kumral, M., Karakaya, N., Karakaya, M. C. and Yildirim, D. K. 2015. A Windows program for chlorite calculation and classification. *Computers and Geosciences*, **81**, 101–113.

Zimmer, M., Kröner, A., Jochum, K.P., Reischmann, T. and Todt, W. 1995. The Gabal Gerf complex: a Precambrian N-MORB ophiolite in the Nubian Shield, NE Africa. *Chemical Geology*, **123**, 29–51.

Manuscript submitted: 15th April 2024
Revised version accepted: 27th September 2024

APPENDIX 1

Chemical composition of chlorites in the chloritite and serpentinite

Rock type	Chloritite											
Sample No.	**Br19**											
SiO2	29.13	29.4	28.48	29.68	30.35	28.72	29.68	29.79	28.82	29.45	30.56	30.38
TiO2	0.29	0.41	0.23	0.34	0.36	0.22	0.34	0.43	0.21	0.43	0.36	0.43
Al2O3	14.9	14.4	15.84	14.26	14.95	16.09	14.87	14.64	15.99	13.34	14.49	16.35
Cr2O3	0.23	0.31	0.17	0.62	0.14	0.09	0.25	0.31	0.24	0.19	0.33	0.41
FeO*	27.53	26.55	27.68	25.75	26.29	27.54	25.47	27.67	25.76	25.01	26.42	24.5
MnO	0.56	0.51	0.59	0.51	0.49	0.46	0.54	0.51	0.4	0.54	0.49	0.53
MgO	9.48	9.53	10.2	11.71	9.34	10.1	10.52	9.45	11.62	11.35	10.43	10.56
NiO	0.11	0.06	0.9	0.13	0.06	0.14	0.05	0.21	0.14	0.06	0.15	0.12
CaO	0.82	0.78	0.95	0.31	0.35	0.97	0.65	0.43	0.33	1.51	0.27	0.76
Na2O	0.24	0.18	0.25	0.12	0.09	0.25	0.18	0.1	0.1	0.34	0.12	0.22
K2O	1.11	1.81	0.45	1.21	1.23	0.59	1	0.56	0.43	0.53	0.57	0.74
P2O5	0.01	0.02	0.01	<dl	0.01	0.01	<dl	0.01	<dl	<dl	<dl	<dl
Total	84.41	83.96	85.75	84.63	83.66	85.18	83.54	84.1	84.04	82.75	84.18	85.01
Structural formula on the basis of 28 oxygen atoms												
Si	6.443	6.515	6.238	6.482	6.654	6.282	6.527	6.569	6.310	6.573	6.658	6.481
Al vi	2.383	2.338	2.365	2.200	2.587	2.477	2.439	2.428	2.479	2.123	2.435	2.662
Ti	0.047	0.068	0.039	0.056	0.059	0.037	0.056	0.071	0.034	0.072	0.059	0.070
Cr	0.040	0.054	0.029	0.107	0.024	0.016	0.043	0.054	0.042	0.034	0.057	0.069
Fe3+	0.355	0.327	0.295	0.336	0.607	0.356	0.472	0.581	0.431	0.361	0.620	0.627
Fe2+	4.737	4.594	4.776	4.367	4.213	4.683	4.212	4.522	4.285	4.307	4.194	3.745
Mn	0.105	0.096	0.109	0.094	0.091	0.085	0.101	0.095	0.074	0.102	0.090	0.096
Mg	3.126	3.148	3.330	3.812	3.052	3.293	3.449	3.106	3.792	3.776	3.387	3.358
Ni	0.020	0.011	0.159	0.023	0.011	0.025	0.009	0.037	0.025	0.011	0.026	0.021
Ca	0.194	0.185	0.223	0.073	0.082	0.227	0.153	0.102	0.077	0.361	0.063	0.174
Na	0.206	0.155	0.212	0.102	0.077	0.212	0.154	0.086	0.085	0.294	0.101	0.182
K	0.626	1.023	0.251	0.671	0.688	0.326	0.558	0.312	0.237	0.302	0.314	0.403
Variety	Diabantite	Diabantite	Diabantite	Diabantite	Diabantite	Diabantite	Diabantite	Diabantite	Diabantite	Diabantite	Diabantite	Diabantite
T ºC	**229**	**221**	**250**	**220**	**206**	**245**	**217**	**216**	**238**	**210**	**204**	**221**

Appendix 1. Cont.

Rock type	Chloritite												
Sample No.	**Chl5**												
SiO2	30.67	30.57	30.4	29.29	31.59	29.37	29.27	30.06	29.66	30.17	30.43	29.44	30.6
TiO2	0.27	0.48	0.41	0.4	0.44	0.36	0.22	0.26	0.3	0.29	0.36	0.34	0.28
Al2O3	16.08	15.62	16.09	15.16	16.61	16.36	14.97	14.65	18.39	16.66	15.05	15.79	14.08
Cr2O3	0.17	0.36	0.28.	0.18	0.26	0.35	0.37	0.81	0.43	1.68	1	0.41	1.25
FeO*	25.45	25.12	25.96	26.11	24.28	25.42	25.95	26.36	25.98	25.93	26.48	26	26.61
MnO	0.46	0.55	0.5	0.47	0.48	0.55	0.04	0.04	0.05	0.04	0.04	0.04	0.04
MgO	9.22	9.69	9.45	11.27	9.66	11.07	12.28	11.31	10.41	10.68	10.59	11.07	10.39
NiO	0.08	0.07	0.21	0.13	0.17	0.09	0.18	0.2	0.18	0.25	0.19	0.18	0.21
CaO	0.36	0.93	0.66	0.38	0.23	0.46	0.16	0.02	0.31	0.02	0.24	0.15	0.13
Na2O	0.09	0.21	0.15	0.22	0.08	0.17	0.05	0.04	0.03	0.08	0.11	0.09	0.07
K2O	0.38	0.25	0.77	0.74	0.64	0.47	0.12	0.07	0.09	0.14	0.22	0.11	0.08
P2O5	0.01	0.01	0.02	0.01	<dl	<dl	<dl	<dl	<dl	<dl	<dl	<dl	<dl
Total	83.24	83.85	84.61	84.35	84.44	84.67	83.62	83.83	85.83	85.94	84.71	83.62	83.74
Structural formula on the basis of 28 oxygen atoms													
Si	6.664	6.616	6.543	6.407	6.694	6.348	6.428	6.568	6.269	6.391	6.571	6.434	6.692
Al vi	2.856	2.667	2.692	2.364	2.926	2.571	2.341	2.388	2.914	2.613	2.458	2.552	2.374
Ti	0.044	0.077	0.066	0.065	0.070	0.058	0.037	0.043	0.048	0.047	0.058	0.056	0.046
Cr	0.029	0.062	0.048	0.031	0.044	0.060	0.064	0.140	0.072	0.281	0.171	0.071	0.216
Fe3+	0.852	0.770	0.671	0.391	0.917	0.523	0.484	0.647	0.736	0.739	0.691	0.623	0.749
Fe2+	3.772	3.776	4.002	4.386	3.386	4.072	4.282	4.170	3.857	3.855	4.091	4.129	4.118

Mn	0.085	0.101	0.091	0.087	0.086	0.101	0.007	0.007	0.009	0.007	0.007	0.007	0.007
Mg	2.986	3.126	3.032	3.675	3.051	3.567	4.020	3.684	3.280	3.373	3.409	3.607	3.387
Ni	0.014	0.012	0.036	0.023	0.029	0.016	0.032	0.035	0.031	0.043	0.033	0.032	0.037
Ca	0.084	0.216	0.152	0.089	0.052	0.107	0.038	0.005	0.070	0.004	0.056	0.035	0.030
Na	0.076	0.176	0.125	0.187	0.066	0.142	0.043	0.034	0.025	0.066	0.092	0.076	0.059
K	0.211	0.138	0.420	0.413	0.347	0.259	0.067	0.039	0.049	0.076	0.121	0.061	0.045
Variety	Diabantite	Diabantite	Diabantite	Diabantite	Diabantite	Diabantite	Diabantite	Diabantite	Diabantite	Diabantite	Diabantite	Diabantite	Diabantite
T ºC	**205**	**209**	**217**	**229**	**200**	**235**	**225**	**212**	**245**	**231**	**213**	**226**	**200**

Appendix 1. Cont.

Rock type	**Serpentinite**												
Sample No.	**SRP2**												
SiO2	25.04	25.22	25.42	25.31	25.57	26.31	24.84	26.6	26.84	25.87	25.55	25.49	25.11
TiO2	0.28	0.84	0.21	0.21	0.14	0.07	0.21	0.49	0.28	0.07	0.42	0.56	0.21
Al2O3	21.7	20.89	20.6	22.66	21.92	21.75	21.32	20.25	22.68	21.21	21.25	20.88	21.46
Cr2O3	0.08	0.12	0.23	0.17	0.09	0.11	0.22	0.14	0.19	0.08	0.06	0.02	0.09
FeO*	15.88	16.03	15.99	16.35	16.48	15.92	16.13	15.53	15.87	15.63	15.78	15.83	16.09
MnO	0.35	0.31	0.35	0.4	0.35	0.33	0.32	0.38	0.37	0.39	0.34	0.33	0.36
MgO	20.8	21.11	20.6	20.16	20.46	20.85	21.65	22.68	21.77	20.57	20.95	21.18	20.35
NiO	0.05	0.11	0.06	0.05	0.04	0.02	0.07	0.11	0.17	0.21	0.04	0.06	0.07
CaO	0.01	0.03	0.12	0.21	0.08	0.01	0.04	0.02	0.12	0.09	0.02	0.01	0.13
Na2O	0.01	0.02	0.03	0.04	0.02	0.01	0.03	0.03	0.03	0.06	0.01	0.02	0.04
K2O	0.01	0.01	0.02	0.1	0.01	<dl	<dl	0.01	0.01	0.03	0.01	0.01	0.02
P2O5	<dl	<dl	0.01	0.02	<dl	<dl	<dl	<dl	0.02	<dl	<dl	<dl	0.01
Total	84.21	84.69	83.64	85.68	85.16	85.38	84.83	86.24	88.35	84.21	84.43	84.39	83.94
Structural formula on the basis of 28 oxygen atoms													
Si	5.242	5.262	5.369	5.220	5.304	5.409	5.158	5.418	5.333	5.406	5.331	5.325	5.284
Al vi	2.602	2.404	2.502	2.734	2.665	2.686	2.405	2.290	2.650	2.636	2.558	2.470	2.612
Ti	0.044	0.132	0.033	0.033	0.022	0.011	0.033	0.075	0.042	0.011	0.066	0.088	0.033
Cr	0.013	0.020	0.038	0.028	0.015	0.018	0.036	0.023	0.030	0.013	0.010	0.003	0.015
Fe3+	0.000	0.000	0.000	0.007	0.011	0.072	0.000	0.000	0.047	0.028	0.014	0.000	0.000
Fe2+	2.805	2.822	2.840	2.813	2.848	2.665	2.946	2.700	2.590	2.703	2.740	2.780	2.849
Mn	0.062	0.055	0.063	0.070	0.061	0.057	0.056	0.066	0.062	0.069	0.060	0.058	0.064
Mg	6.491	6.565	6.486	6.198	6.326	6.389	6.702	6.886	6.448	6.408	6.516	6.596	6.384
Ni	0.008	0.018	0.010	0.008	0.007	0.003	0.012	0.018	0.027	0.035	0.007	0.010	0.012
Ca	0.002	0.007	0.027	0.046	0.018	0.002	0.009	0.004	0.026	0.020	0.004	0.002	0.029
Na	0.008	0.016	0.025	0.032	0.016	0.008	0.024	0.024	0.023	0.049	0.008	0.016	0.033
K	0.005	0.005	0.011	0.053	0.005	0.000	0.000	0.005	0.005	0.016	0.005	0.005	0.011
Variety	ripidolite	ripidolite	ripidolite	ripidolite	ripidolite	ripidolite	ripidolite	ripidolite	ripidolite	ripidolite	ripidolite	ripidolite	ripidolite
T ºC	**333**	**331**	**319**	**336**	**327**	**315**	**342**	**313**	**322**	**315**	**323**	**324**	**329**

Appendix 1. Cont.

Rock type	**Serpentinite**												
Sample No.	**SRP2**												
SiO2	24.23	25.38	25.67	25.83	26.48	26.28	26.01	25.96	24.74	26.08	25.53	23.66	25.5
TiO2	0.14	0.14	0.14	0.35	0.35	0.42	0.84	0.14	0.14	0.56	0.28	0.14	0.35
Al2O3	21.6	21.98	21.94	21.24	21.49	21.26	22.18	21.28	21.46	21.59	21.36	20.02	21.28
Cr2O3	0.21	0.33	0.16	0.12	0.09	0.5	0.7	0.06	0.12	0.18	0.24	0.08	0.31
FeO*	16.39	16.27	15.97	15.86	16.01	15.99	15.91	15.61	15.96	16.16	15.95	15.94	15.82
MnO	0.38	0.35	0.34	0.32	0.37	0.37	0.39	0.38	0.34	0.35	0.36	0.36	0.36
MgO	20.08	20.62	21.01	21.64	21.02	21.33	21.43	20.97	20.27	20.25	20.91	20.76	20.89
NiO	0.14	0.17	0.06	0.09	0.04	0.12	0.16	0.09	0.07	0.15	0.18	0.21	0.05
CaO	0.18	0.1	0.03	0.04	0.04	0.09	0.08	0.07	<dl	0.09	0.1	0.1	0.11
Na2O	0.05	0.03	0.02	0.04	0.02	0.03	0.02	0.04	<dl	0.04	0.02	0.03	0.05
K2O	0.06	0.02	<dl	0.01	0.02	0.02	0	0.02	<dl	0.03	0.02	0.01	0.03
P2O5	0.01	<dl	<dl	<dl	<dl	<dl	0.01	<dl	<dl	0.01	<dl	<dl	0.01

Total	83.47	85.39	85.34	85.54	85.93	86.41	87.73	84.62	83.1	85.49	84.95	81.31	84.76
Structural formula on the basis of 28 oxygen atoms													
Si	5.138	5.253	5.300	5.315	5.414	5.364	5.229	5.394	5.257	5.371	5.305	5.138	5.307
Al vi	2.560	2.621	2.640	2.475	2.602	2.482	2.490	2.609	2.636	2.623	2.542	2.303	2.532
Ti	0.022	0.022	0.022	0.054	0.054	0.064	0.127	0.022	0.022	0.087	0.044	0.023	0.055
Cr	0.035	0.054	0.026	0.020	0.015	0.081	0.111	0.010	0.020	0.029	0.039	0.014	0.051
Fe3+	0.000	0.000	0.002	0.000	0.071	0.023	0.043	0.022	0.000	0.098	0.000	0.000	0.000
Fe2+	3.012	2.834	2.756	2.770	2.667	2.706	2.632	2.691	2.854	2.685	2.787	3.109	2.763
Mn	0.068	0.061	0.059	0.056	0.064	0.064	0.066	0.067	0.061	0.061	0.063	0.066	0.063
Mg	6.347	6.362	6.466	6.638	6.407	6.490	6.423	6.495	6.421	6.217	6.478	6.720	6.481
Ni	0.024	0.028	0.010	0.015	0.007	0.020	0.026	0.015	0.012	0.025	0.030	0.037	0.008
Ca	0.041	0.022	0.007	0.009	0.009	0.020	0.017	0.016	0.000	0.020	0.022	0.023	0.025
Na	0.041	0.024	0.016	0.032	0.016	0.024	0.016	0.032	0.000	0.032	0.016	0.025	0.040
K	0.032	0.011	0.000	0.005	0.010	0.010	0.000	0.011	0.000	0.016	0.011	0.006	0.016
Variety	ripidolite	ripidolite	ripidolite	ripidolite	ripidolite	ripidolite	ripidolite	ripidolite	ripidolite	ripidolite	ripidolite	ripidolite	ripidolite
T ^{o}C	**345**	**332**	**326**	**324**	**314**	**319**	**334**	**316**	**332**	**320**	**326**	**345**	**326**

Appendix 1. Cont.

Rock type	**Serpentinite**											
Sample No.	**SRP2**											
SiO2	25.02	25.23	25.6	25.64	26.88	26.41	26.21	26.85	25.69	26.36	24.58	25.96
TiO2	0.28	0.14	0.07	0.21	0.42	0.14	0.35	1.4	0.21	0.14	0.63	0.35
Al2O3	21.97	21.66	22.47	21.59	21.34	21.86	22.24	21.66	21.83	21.39	20.49	20.95
Cr2O3	0.27	0.19	0.14	0.16	0.08	0.07	0.21	0.13	0.17	0.08	0.06	0.09
FeO*	16.22	15.81	16.1	15.67	15.86	16.28	16.27	15.85	15.88	15.48	15.96	15.8
MnO	0.37	0.34	0.34	0.3	0.37	0.37	0.37	0.4	0.39	0.36	0.38	0.36
MgO	20.63	21.26	20.57	21.21	21.3	20.24	20.27	21.57	21.21	21.46	20.93	21.98
NiO	0.12	0.09	0.14	0.06	0.04	0.08	0.21	0.02	0.7	0.12	0.18	0.23
CaO	0.05	0.07	0.03	0.05	0.05	0.09	0.08	0.04	0.06	0.08	0.09	0.03
Na2O	0.02	0.04	0.02	0.03	0.04	0.03	<dl	0.02	<dl	0.03	0.05	0.04
K2O	<dl	0.02	0.01	0.02	0.02	0.02	0.03	0.02	<dl	0.02	0.02	<dl
P2O5	<dl	<dl	<dl	<dl	<dl	<dl	<dl	0.01	<dl	<dl	<dl	<dl
Total	84.95	84.85	85.49	84.94	86.4	85.59	86.24	87.97	86.14	85.52	83.37	85.79
Structural formula on the basis of 28 oxygen atoms												
Si	5.205	5.234	5.275	5.311	5.456	5.423	5.349	5.353	5.269	5.411	5.208	5.325
Al vi	2.599	2.545	2.737	2.586	2.572	2.725	2.709	2.455	2.553	2.590	2.348	2.404
Ti	0.044	0.022	0.011	0.033	0.064	0.022	0.054	0.210	0.032	0.022	0.100	0.054
Cr	0.044	0.031	0.023	0.026	0.013	0.011	0.034	0.020	0.028	0.013	0.010	0.015
Fe3+	0.000	0.000	0.027	0.000	0.084	0.104	0.107	0.132	0.000	0.024	0.000	0.000
Fe2+	2.852	2.812	2.748	2.725	2.608	2.691	2.670	2.511	2.760	2.634	2.935	2.778
Mn	0.065	0.060	0.059	0.053	0.064	0.064	0.064	0.068	0.068	0.063	0.068	0.063
Mg	6.398	6.574	6.319	6.549	6.445	6.195	6.166	6.410	6.484	6.566	6.611	6.721
Ni	0.020	0.015	0.023	0.010	0.007	0.013	0.034	0.003	0.115	0.020	0.031	0.038
Ca	0.011	0.016	0.007	0.011	0.011	0.020	0.017	0.009	0.013	0.018	0.020	0.007
Na	0.016	0.032	0.016	0.024	0.031	0.024	0.000	0.015	0.000	0.024	0.041	0.032
K	0.000	0.011	0.005	0.011	0.010	0.010	0.016	0.010	0.000	0.010	0.011	0.000
Variety	ripidolite	ripidolite	ripidolite	ripidolite	ripidolite	ripidolite	ripidolite	ripidolite	ripidolite	ripidolite	ripidolite	ripidolite
T ^{o}C	**337**	**333**	**329**	**325**	**310**	**314**	**322**	**320**	**330**	**314**	**337**	**323**

APPENDIX 2

Chemical composition of annite in the chloritite

Sample No.	Br19										
Spot No.	**Ann1**	**Ann2**	**Ann3**	**Ann4**	**Ann5**	**Ann6**	**Ann7**	**Ann8**	**Ann9**	**Ann10**	**Ann11**
SiO2	35.91	36.22	37	36.38	36	36.19	36.8	36.86	36.82	37.05	36.79
TiO2	2.44	2.84	3.15	2.96	2.54	2.66	3.26	3.24	3.04	3.09	2.98
Al2O3	12.19	11.87	12.1	11.66	12.14	11.69	12.03	12.11	12.21	11.99	11.96
Cr2O3	<dl	<dl	0.01	0.01	<dl	<dl	<dl	<dl	0.01	<dl	0.01
FeO*	21.4	20.37	20.91	21.06	21.21	20	19.87	20.17	20.93	21.11	21.22
MnO	0.51	0.5	0.47	0.45	0.52	0.52	0.51	0.5	0.48	0.45	0.47
MgO	10.81	10.96	11.16	10.69	10.73	11.2	11.21	11.19	10.61	11.17	10.69
NiO	0.02	0.01	0.01	<dl	0.01	<dl	0.01	0.01	<dl	<dl	<dl
CaO	0.1	0.07	0.12	0.15	0.08	0.03	0.09	0.09	0.12	0.11	0.15
Na2O	0.12	0.1	0.17	0.18	0.1	0.1	0.13	0.14	0.1	0.2	0.17
K2O	7.83	9.14	9.13	8.77	8.18	9.17	9.07	9.15	9.02	9.18	8.98
P2O5	0.02	<dl	<dl	0.01	0.01	0.01	0.01	0.01	<dl	<dl	0.01
Total	91.35	92.08	94.23	92.32	91.52	91.57	92.99	93.47	93.34	94.35	93.43
Structural formula on the basis of 22 oxygen atoms											
Si	5.715	5.724	5.695	5.738	5.721	5.746	5.718	5.706	5.722	5.701	5.725
Al iv	2.285	2.211	2.195	2.168	2.274	2.188	2.203	2.210	2.237	2.175	2.194
Al vi	0.002	0.000	0.000	0.000	0.000	0.000	0.000	0.000	0.000	0.000	0.000
Ti	0.292	0.338	0.365	0.351	0.304	0.318	0.381	0.377	0.355	0.358	0.349
Cr	0.000	0.000	0.001	0.001	0.000	0.000	0.000	0.000	0.001	0.000	0.001
Fe	2.848	2.692	2.692	2.778	2.819	2.656	2.582	2.611	2.720	2.717	2.762
Mn	0.069	0.067	0.061	0.060	0.070	0.070	0.067	0.066	0.063	0.059	0.062
Mg	2.565	2.582	2.561	2.513	2.542	2.651	2.597	2.582	2.458	2.562	2.480
Ni	0.003	0.001	0.001	0.000	0.001	0.000	0.001	0.001	0.000	0.000	0.000
Ca	0.017	0.012	0.020	0.025	0.014	0.005	0.015	0.015	0.020	0.018	0.025
Na	0.037	0.031	0.051	0.055	0.031	0.031	0.039	0.042	0.030	0.060	0.051
K	1.589	1.843	1.792	1.764	1.658	1.857	1.798	1.807	1.788	1.802	1.782

Appendix 2. Cont.

Sample No.	CHL5									
Spot No.	**Ann1**	**Ann2**	**Ann3**	**Ann4**	**Ann5**	**Ann6**	**Ann7**	**Ann8**	**Ann9**	**Ann10**
SiO2	36.2	35.03	37.17	36.29	35.69	37.12	36.74	36.64	36.03	35.32
TiO2	2.72	2.7	3.25	2.95	2.84	3.06	2.82	2.49	3.2	2.92
Al2O3	11.75	11.26	12.13	12.07	11.41	12.1	12.04	12.25	11.76	11.2
Cr2O3	<dl	<dl	<dl	<dl	<dl	<dl	<dl	<dl	<dl	<dl
FeO*	21.63	23.09	19.82	20.41	20.06	20.94	21.65	21.68	20.69	22.76
MnO	0.44	0.49	0.51	0.54	0.48	0.48	0.46	0.44	0.5	0.52
MgO	10.81	10.07	11.29	10.86	11.6	10.91	9.99	11	11.23	9.85
NiO	<dl	0.01	0.01	<dl	<dl	<dl	<dl	0.01	<dl	0.01
CaO	0.17	0.33	0.1	<dl	<dl	<dl	<dl	0.22	0.11	0.31
Na2O	0.18	0.19	0.1	0.1	0.14	0.15	0.09	0.18	0.19	0.18
K2O	8.36	7.71	9.13	9.13	9.08	9.18	9.02	7.69	9.09	7.9
P2O5	0.01	<dl	0.02	<dl	<dl	0.01	0.01	0.01	<dl	<dl
Total	92.27	90.88	93.53	92.35	91.3	93.95	92.82	92.61	92.8	90.97
Structural formula on the basis of 22 oxygen atoms										
Si	5.721	5.699	5.727	5.711	5.703	5.720	5.759	5.723	5.669	5.725
Al iv	2.189	2.159	2.203	2.239	2.149	2.198	2.225	2.255	2.181	2.140
Al vi	0.000	0.000	0.000	0.000	0.000	0.000	0.000	0.000	0.000	0.000
Ti	0.323	0.330	0.377	0.349	0.341	0.355	0.332	0.293	0.379	0.356
Cr	0.000	0.000	0.000	0.000	0.000	0.000	0.000	0.000	0.000	0.000

Fe	2.859	3.141	2.554	2.686	2.681	2.699	2.838	2.832	2.723	3.085
Mn	0.059	0.068	0.067	0.072	0.065	0.063	0.061	0.058	0.067	0.071
Mg	2.547	2.442	2.593	2.548	2.763	2.506	2.334	2.561	2.634	2.380
Ni	0.000	0.001	0.001	0.000	0.000	0.000	0.000	0.001	0.000	0.001
Ca	0.029	0.058	0.017	0.010	0.010	0.020	0.018	0.037	0.019	0.054
Na	0.055	0.060	0.030	0.031	0.043	0.045	0.027	0.055	0.058	0.057
K	1.685	1.600	1.794	1.833	1.851	1.804	1.803	1.532	1.824	1.633

APPENDIX 3

Chemical composition of chrome spinel and its alteration in the serpentinites

Sample No.	**SRP-2**											
Mineral	**Fresh chrome spinel**											
Spot No.	**Sp1**	**Sp2**	**Sp3**	**Sp4**	**Sp5**	**Sp6**	**Sp7**	**Sp8**	**Sp9**	**Sp10**	**Sp11**	**Sp12**
SiO2	0.08	0.03	0.05	0.03	0.03	0.02	0.06	0.03	0.07	0.06	0.03	0.04
TiO2	0.13	0.08	0.11	0.08	0.1	0.08	0.07	0.08	0.09	0.11	0.09	0.08
Al2O3	20.2	17.55	17.52	16.75	16.16	14.56	12.61	13.72	12.97	18.1	16.06	14.12
Cr2O3	48.33	49.49	50.03	50.51	51.56	52.73	55.4	55.03	55.96	49.89	51.54	53.99
FeO	18.3	21.51	19.86	21.46	20.73	21.44	23.67	22.74	20.74	19.89	20.96	22.34
MnO	0.5	0.52	0.51	0.45	0.5	0.47	0.55	0.53	0.55	0.51	0.47	0.52
MgO	11.65	9.78	11.28	9.82	10.13	9.3	6.42	7.36	8.7	10.51	10.07	8.01
CaO	0.02	0.01	0.01	0.02	0.02	0.02	0.02	0.03	0.06	0.03	0.01	0.02
Na2O	0.01	0.03	0.03	0.02	0.01	0.03	0.02	0.01	0.01	0.02	0.02	0.02
K2O	0.04	0.07	0.11	0.07	0.02	0.02	0.04	0.03	0.04	0.05	0.06	0.03
P2O5	0.09	0.08	0.04	0.08	0.05	0.03	0.04	0.04	0.04	0.08	0.05	0.04
NiO	0.14	0.12	0.09	0.13	0.11	0.1	0.06	0.06	0.05	0.12	0.09	0.08
Total	99.5	99.27	99.62	99.39	99.39	98.77	98.94	99.63	99.25	99.34	99.45	99.28
Structural formula on the basis of 4 oxygen atoms												
Ti	0.003	0.002	0.003	0.002	0.002	0.002	0.002	0.002	0.002	0.003	0.002	0.002
Al	0.749	0.667	0.657	0.638	0.615	0.565	0.503	0.538	0.507	0.683	0.612	0.552
Cr	1.203	1.263	1.260	1.291	1.317	1.372	1.483	1.447	1.468	1.263	1.318	1.415
Fe3+	0.042	0.066	0.078	0.067	0.062	0.060	0.010	0.012	0.020	0.049	0.065	0.030
Fe2+	0.440	0.514	0.451	0.513	0.498	0.530	0.660	0.621	0.555	0.484	0.501	0.590
Mn	0.013	0.014	0.014	0.012	0.014	0.013	0.016	0.015	0.015	0.014	0.013	0.015
Ni	0.004	0.003	0.002	0.003	0.003	0.003	0.002	0.002	0.001	0.003	0.002	0.002
Mg	0.547	0.470	0.535	0.473	0.488	0.456	0.324	0.365	0.430	0.502	0.486	0.396
Cr#	0.62	0.65	0.66	0.67	0.68	0.71	0.75	0.73	0.74	0.65	0.68	0.72
Mg#	0.55	0.48	0.54	0.48	0.49	0.46	0.33	0.37	0.44	0.51	0.49	0.40

Appendix 3. Cont.

Sample No.	**SRP-2**											
Mineral	**Fresh chrome spinel**					**Ferritchromite**						
Spot No.	**Sp13**	**Sp14**	**Sp15**	**Sp16**	**Sp17**	**Fe-Cr**	**Fe-Cr**	**Fe-Cr**	**Fe-Cr**	**Fe-Cr**	**Fe-Cr**	**Fe-Cr**
SiO2	0.06	0.05	0.02	0.03	0.05	0.13	0.14	0.19	0.2	0.14	0.16	0.14
TiO2	0.11	0.1	0.08	0.09	0.08	0.12	0.17	0.08	0.08	0.14	0.12	0.1
Al2O3	19.36	17.71	16.23	15.67	13.22	1	0.77	1.67	1.92	0.88	1.22	1.51
Cr2O3	48.56	49.82	51.13	53.1	55.49	20.67	29.72	36.15	39.93	25.2	32.94	31.4
FeO	19.56	20.23	21.32	21.81	22.12	74.08	64.19	56.43	52.27	69.14	60.31	60.65
MnO	0.5	0.52	0.43	0.52	0.53	2.37	2.71	2.04	1.92	2.54	2.38	2.34

MgO	10.98	10.73	9.94	8.66	7.77	0.84	1.17	2.8	2.77	1.02	1.98	2.03
CaO	0.02	0.01	0.01	0.02	0.04	0.02	0.01	0.04	0.02	0.01	0.03	0.01
Na2O	0.02	0.03	0.02	0.02	0.01	0.01	0.02	0.04	0.02	0.04	0.03	0.02
K2O	0.06	0.08	0.04	0.03	0.03	0.03	0.02	0.03	0.05	0.02	0.02	0.02
P2O5	0.08	0.07	0.06	0.04	0.04	0.07	0.05	0.06	0.07	0.06	0.05	0.05
NiO	0.13	0.11	0.1	0.1	0.05	0.12	0.15	0.17	0.15	0.13	0.16	0.44
Total	99.44	99.45	99.37	100.1	99.42	99.45	99.11	99.69	99.39	99.31	99.39	98.71
Structural formula on the basis of 4 oxygen atoms												
Ti	0.003	0.002	0.002	0.002	0.002	0.003	0.005	0.002	0.002	0.004	0.003	0.003
Al	0.724	0.668	0.619	0.601	0.519	0.042	0.033	0.070	0.081	0.038	0.052	0.064
Cr	1.218	1.260	1.308	1.366	1.461	0.591	0.856	1.023	1.135	0.723	0.940	0.900
Fe3+	0.053	0.067	0.069	0.028	0.016	1.360	1.102	0.903	0.780	1.232	1.002	1.030
Fe2+	0.466	0.474	0.508	0.565	0.600	0.882	0.853	0.786	0.791	0.867	0.819	0.808
Mn	0.013	0.014	0.012	0.014	0.015	0.073	0.084	0.062	0.058	0.078	0.073	0.072
Ni	0.003	0.003	0.003	0.003	0.001	0.003	0.004	0.005	0.004	0.004	0.005	0.013
Mg	0.519	0.512	0.480	0.420	0.386	0.045	0.063	0.149	0.148	0.055	0.107	0.110
Cr#	0.63	0.65	0.68	0.69	0.74	0.93	0.96	0.94	0.93	0.95	0.95	0.93
Mg#	0.53	0.52	0.49	0.43	0.39	0.05	0.07	0.16	0.16	0.06	0.12	0.12

Appendix 3. Cont.

Sample No.	**SRP-2**												
Mineral	**Ferritchromite**			**Cr-magnetite**									
Spot No.	**Fe-Cr**	**Fe-Cr**	**Fe-Cr**	**Fe-Cr**	**Cr-Mt**	**Cr-Mt**	**Cr-Mt**	**Cr-Mt**	**Cr-Mt**	**Cr-Mt**	**Cr-Mt**	**Cr-Mt**	**Cr-Mt**
SiO2	0.19	0.11	0.14	0.11	0.07	0.08	0.07	0.04	0.09	0.05	0.06	0.01	0.03
TiO2	0.08	0.09	0.1	0.13	0.11	0.05	0.08	0.01	0.02	0.06	0.03	0.02	0.03
Al2O3	1.79	1.39	1.39	0.99	0.15	0.03	0.07	0.05	0.03	0.37	0.24	0.07	0.06
Cr2O3	38.04	37.3	37.54	37.45	7.34	3.15	5.23	3	2.53	17.84	8.2	11.5	5.55
FeO	54.35	52.56	53.34	52.66	85.81	90.06	88.36	88.59	88.61	74.27	82.18	80.87	87.7
MnO	1.98	2.59	2.07	2.64	0.84	0.49	0.68	0.22	0.22	1.01	0.34	0.42	0.38
MgO	2.79	3.96	3.54	3.32	0.22	0.15	0.18	0.96	0.79	2.09	1.71	0.84	0.64
CaO	0.04	0.01	0.02	0.01	0.02	0.01	0.01	0.02	<dl	0.02	0.03	0.01	0.01
Na2O	0.03	0.04	0.02	0.01	0.01	0.03	0.02	0.03	0.03	0.01	0.02	0.04	0.02
K2O	0.04	0.03	0.05	0.02	0.05	0.06	0.04	0.03	0.04	0.01	0.05	0.07	0.06
P2O5	0.07	0.03	0.07	0.05	0.08	0.08	0.08	0.08	0.04	0.01	0.06	0.04	0.03
NiO	0.14	0.23	0.33	0.13	0.12	0.06	0.08	0.61	0.67	0.43	0.44	0.43	0.27
Total	99.53	98.34	98.6	97.51	94.8	94.26	94.91	93.63	93.06	96.17	93.35	94.33	94.77
Structural formula on the basis of 4 oxygen atoms													
Ti	0.002	0.002	0.003	0.004	0.003	0.002	0.002	0.000	0.001	0.002	0.001	0.001	0.001
Al	0.076	0.059	0.059	0.042	0.006	0.001	0.003	0.002	0.001	0.016	0.011	0.003	0.003
Cr	1.079	1.060	1.069	1.081	0.220	0.095	0.157	0.091	0.077	0.522	0.247	0.346	0.166
Fe3+	0.841	0.876	0.867	0.870	1.767	1.901	1.836	1.907	1.921	1.458	1.741	1.649	1.830
Fe2+	0.789	0.705	0.740	0.738	0.960	0.975	0.968	0.920	0.927	0.842	0.879	0.926	0.945
Mn	0.060	0.079	0.063	0.082	0.027	0.016	0.022	0.007	0.007	0.032	0.011	0.014	0.012
Ni	0.004	0.007	0.010	0.004	0.004	0.002	0.002	0.019	0.021	0.013	0.013	0.013	0.008
Mg	0.149	0.212	0.190	0.181	0.012	0.009	0.010	0.054	0.045	0.115	0.097	0.048	0.036
Cr#	0.93	0.95	0.95	0.96	0.97	0.99	0.98	0.98	0.99	0.97	0.96	0.99	0.98
Mg#	0.16	0.23	0.20	0.20	0.01	0.01	0.01	0.06	0.05	0.12	0.10	0.05	0.04

APPENDIX 4

Chemical composition of magnetite in the chloritite

Mineral	**Magnetite**													
Sample No.	**Br19**													
Spot No.	**Mt1**	**Mt2**	**Mt3**	**Mt4**	**Mt5**	**Mt6**	**Mt7**	**Mt8**	**Mt9**	**Mt10**	**Mt11**	**Mt12**	**Mt13**	**Mt14**
SiO2	0.01	0.04	0.03	0.03	0.08	0.16	0.06	0.25	0.01	0.01	0.02	0.16	0.11	0.15
TiO2	0.75	0.12	0.03	0.8	0.03	0.01	0.03	0.48	0.02	0.06	0.03	0.01	0.05	0.58
Al2O3	0.06	0.05	0.08	0.07	0.06	0.06	0.07	0.16	0.04	0.04	0.07	0.24	0.05	0.12
Cr2O3	0.72	1.04	0.92	0.63	0.85	1.07	0.95	0.58	0.89	0.82	0.83	0.84	0.81	0.63
FeO*	92.16	92.9	92.85	92.32	92.98	91.29	92.69	90.48	94.23	93.23	93.04	92.79	93.48	91.92
MnO	0.11	0.09	0.09	0.14	0.07	0.07	0.11	0.06	0.07	0.07	0.08	0.08	0.08	0.09
MgO	0.01	0.14	0.14	0.01	0.16	0.13	0.11	0.01	0.13	0.09	0.09	0.2	0.17	0.01
NiO	0.19	0.3	0.34	0.12	0.3	0.3	0.33	0.12	0.27	0.3	0.31	0.32	0.33	0.27
CaO	0.08	<dl	<dl	0.05	<dl	<dl	<dl	0.04	<dl	<dl	<dl	<dl	<dl	0.05
Na2O	0.01	<dl	<dl	0.01	0.01	<dl	<dl	<dl	<dl	<dl	<dl	0.05	<dl	0.01
K2O	<dl	<dl	<dl	<dl	<dl	<dl	<dl	<dl	<dl	<dl	<dl	<dl	<dl	<dl
P2O5	0.01	<dl	<dl	<dl	<dl	<dl	<dl	<dl	<dl	<dl	0.01	<dl	<dl	<dl
Total	94.11	94.68	94.48	94.18	94.54	93.09	94.35	92.18	95.66	94.62	94.48	94.69	95.08	93.83
Structural formula on the basis of 4 oxygen atoms														
Si	0.000	0.002	0.001	0.001	0.003	0.006	0.002	0.010	0.000	0.000	0.001	0.006	0.004	0.006
Ti	0.022	0.003	0.001	0.023	0.001	0.000	0.001	0.014	0.001	0.002	0.001	0.000	0.001	0.017
Al	0.003	0.002	0.004	0.003	0.003	0.003	0.003	0.007	0.002	0.002	0.003	0.011	0.002	0.005
Fe+3	1.929	1.952	1.960	1.928	1.959	1.947	1.957	1.925	1.966	1.965	1.964	1.946	1.957	1.926
Fe+2	1.013	0.992	0.989	1.016	0.990	0.994	0.991	1.019	0.989	0.992	0.992	0.990	0.991	1.015
Mn	0.004	0.003	0.003	0.005	0.002	0.002	0.004	0.002	0.002	0.002	0.003	0.003	0.003	0.003
Mg	0.001	0.008	0.008	0.001	0.009	0.007	0.006	0.001	0.007	0.005	0.005	0.011	0.010	0.001
Ca	0.003	0.000	0.000	0.002	0.000	0.000	0.000	0.002	0.000	0.000	0.000	0.000	0.000	0.002
Na	0.001	0.000	0.000	0.001	0.001	0.000	0.000	0.000	0.000	0.000	0.000	0.004	0.000	0.001
K	0.000	0.000	0.000	0.000	0.000	0.000	0.000	0.000	0.000	0.000	0.000	0.000	0.000	0.000
Cr	0.022	0.031	0.028	0.019	0.025	0.033	0.029	0.018	0.026	0.025	0.025	0.025	0.024	0.019
Ni	0.006	0.009	0.010	0.004	0.009	0.009	0.010	0.004	0.008	0.009	0.009	0.010	0.010	0.008
Mol % Usp														
Stormer (1983)	0.02	0.00	0.00	0.02	0.00	0.00	0.00	0.01	0.00	0.00	0.00	0.00	0.00	0.02

Appendix 4. Cont.

Mineral	**Magnetite**										
Sample No.	**CHL5**										
Spot No.	**Mt1**	**Mt2**	**Mt3**	**Mt4**	**Mt5**	**Mt6**	**Mt7**	**Mt8**	**Mt9**	**Mt10**	**Mt11**
SiO2	0.08	0.19	0.06	0.06	0.09	0.03	0.07	0.02	0.21	0.34	0.02
TiO2	0.04	0.02	0.59	0.12	0.01	0.68	0.04	0.01	0.02	0.04	0.04
Al2O3	0.03	0.09	0.07	0.07	0.02	0.07	0.04	0.06	0.02	0.46	0.05
Cr2O3	0.73	1.03	0.77	0.9	0.87	0.71	0.85	0.76	0.74	0.7	0.95
FeO*	92.55	91.21	91.9	92.88	93.96	92.5	93.62	92.71	92.88	93.54	93.61
MnO	0.06	0.06	0.08	0.09	0.06	0.1	0.07	0.08	0.06	0.08	0.09
MgO	0.17	0.15	0.01	0.08	0.13	0.01	0.14	0.08	0.13	0.3	0.13
NiO	0.28	0.32	0.21	0.33	0.28	0.15	0.33	0.32	0.27	0.29	0.31
CaO	<dl	<dl	0.07	<dl	<dl	0.07	<dl	<dl	<dl	<dl	<dl
Na2O	0.02	<dl	0.01	<dl	<dl	<dl	<dl	0.01	0.01	0.11	<dl
K2O	<dl	<dl	<dl	<dl	<dl	<dl	<dl	<dl	<dl	<dl	<dl
P2O5	<dl	<dl	0.01	<dl	<dl	<dl	0.01	<dl	<dl	<dl	<dl
Total	93.96	93.07	93.78	94.53	95.42	94.32	95.17	94.05	94.34	95.86	95.2
Structural formula on the basis of 4 oxygen atoms											
Si	0.003	0.007	0.002	0.002	0.003	0.001	0.003	0.001	0.008	0.013	0.001
Ti	0.001	0.001	0.017	0.003	0.000	0.019	0.001	0.000	0.001	0.001	0.001
Al	0.001	0.004	0.003	0.003	0.001	0.003	0.002	0.003	0.001	0.020	0.002
Fe+3	1.964	1.944	1.932	1.953	1.962	1.932	1.960	1.967	1.955	1.925	1.961
Fe+2	0.990	0.995	1.012	0.996	0.992	1.013	0.991	0.991	0.997	0.991	0.989
Mn	0.002	0.002	0.003	0.003	0.002	0.003	0.002	0.003	0.002	0.003	0.003
Mg	0.010	0.009	0.001	0.005	0.007	0.001	0.008	0.005	0.007	0.017	0.007
Ca	0.000	0.000	0.003	0.000	0.000	0.003	0.000	0.000	0.000	0.000	0.000
Na	0.001	0.000	0.001	0.000	0.000	0.000	0.000	0.001	0.001	0.008	0.000
K	0.000	0.000	0.000	0.000	0.000	0.000	0.000	0.000	0.000	0.000	0.000
Cr	0.022	0.031	0.023	0.027	0.026	0.021	0.025	0.023	0.022	0.021	0.028
Ni	0.009	0.010	0.006	0.010	0.008	0.005	0.010	0.010	0.008	0.009	0.009
Mol % Usp											
Stormer (1983)	0.00	0.00	0.02	0.00	0.00	0.02	0.00	0.00	0.00	0.00	0.00

Appendix 4. Cont.

Mineral	Cr-Magnetite											
Sample No.	Br19											
Spot No.	**Mt1**	**Mt2**	**Mt3**	**Mt4**	**Mt5**	**Mt6**	**Mt7**	**Mt8**	**Mt9**	**Mt10**	**Mt11**	**Mt12**
SiO2	0.18	0.12	0.06	0.16	0.04	0.11	0.12	0.02	0.07	0.13	0.15	0.12
TiO2	0.05	0.02	0.04	0.12	0.05	0.05	0.12	0.02	0.04	0.13	0.15	0.07
Al2O3	0.06	0.05	0.05	0.07	0.09	0.07	0.06	0.05	0.05	0.08	0.12	0.05
Cr2O3	4.29	3.25	3.56	5.44	4.71	4.84	4.81	3.35	3.79	5.78	8.62	4.31
FeO*	90.32	91.07	90.77	88.5	88.93	89.66	89.61	91.09	90.53	88.12	84.93	89.61
MnO	0.16	0.12	0.15	0.29	0.24	0.23	0.19	0.11	0.16	0.33	0.52	0.18
MgO	0.2	0.18	0.18	0.23	0.18	0.21	0.22	0.18	0.19	0.22	0.29	0.21
NiO	0.34	0.31	0.31	0.34	0.36	0.35	0.35	0.31	0.32	0.33	0.36	0.35
CaO	<dl	<dl	<dl	<dl	<dl	<dl	<dl	<dl	<dl	<dl	<dl	<dl
Na2O	<dl	<dl	<dl	<dl	0.03	<dl	<dl	<dl	<dl	<dl	<dl	0.02
K2O	<dl	<dl	<dl	<dl	<dl	<dl	<dl	<dl	<dl	<dl	<dl	<dl
P2O5	<dl	<dl	<dl	<dl	<dl	<dl	<dl	<dl	<dl	<dl	<dl	<dl
Total	95.6	95.12	95.12	95.15	94.63	95.52	95.48	95.13	95.15	95.12	95.14	94.92
Structural formula on the basis of 4 oxygen atoms												
Si	0.007	0.005	0.002	0.006	0.002	0.004	0.005	0.001	0.003	0.005	0.006	0.005
Ti	0.001	0.001	0.001	0.003	0.001	0.001	0.003	0.001	0.001	0.004	0.004	0.002
Al	0.003	0.002	0.002	0.003	0.004	0.003	0.003	0.002	0.002	0.004	0.005	0.002
Fe+3	1.848	1.886	1.880	1.810	1.843	1.837	1.833	1.890	1.872	1.802	1.712	1.850
Fe+2	0.989	0.989	0.986	0.985	0.982	0.984	0.987	0.985	0.986	0.983	0.974	0.986
Mn	0.005	0.004	0.005	0.009	0.008	0.007	0.006	0.004	0.005	0.011	0.017	0.006
Mg	0.011	0.010	0.010	0.013	0.010	0.012	0.012	0.010	0.011	0.012	0.016	0.012
Ca	0.000	0.000	0.000	0.000	0.000	0.000	0.000	0.000	0.000	0.000	0.000	0.000
Na	0.000	0.000	0.000	0.000	0.000	0.000	0.000	0.000	0.000	0.000	0.000	0.001
K	0.000	0.000	0.000	0.000	0.000	0.000	0.000	0.000	0.000	0.000	0.000	0.000
Cr	0.127	0.097	0.106	0.162	0.141	0.144	0.143	0.100	0.113	0.173	0.258	0.129
Ni	0.010	0.009	0.009	0.010	0.011	0.011	0.011	0.009	0.010	0.010	0.011	0.011
Mol % Usp *Stormer (1983)*	0.00	0.00	0.00	0.00	0.00	0.00	0.00	0.00	0.00	0.00	0.01	0.00

Appendix 4. Cont.

Mineral	Cr-Magnetite								
Sample No.	CHL5								
Spot No.	**Mt1**	**Mt2**	**Mt3**	**Mt4**	**Mt6**	**Mt7**	**Mt8**	**Mt9**	**Mt10**
SiO2	0.11	0.06	0.05	0.07	0.05	0.04	0.14	0.21	0.08
TiO2	0.06	0.16	0.06	0.03	0.09	0.05	0.07	0.03	0.03
Al2O3	0.06	0.08	0.04	0.05	0.11	0.08	0.05	0.05	0.05
Cr2O3	3.95	5.92	4.06	4.09	6.66	5.3	4.45	3.38	3.05
FeO*	89	88.3	90.21	90.59	86.88	88.61	88.99	90.48	89.59
MnO	0.21	0.32	0.16	0.14	0.37	0.2	0.24	0.12	0.12
MgO	0.21	0.23	0.2	0.2	0.23	0.2	0.19	0.17	0.2
NiO	0.35	0.36	0.33	0.33	0.34	0.37	0.36	0.35	0.35
CaO	<dl	<dl	<dl	<dl	<dl	<dl	<dl	<dl	<dl
Na2O	0.01	<dl	0.01	<dl	<dl	0.02	<dl	<dl	<dl
K2O	<dl	<dl	<dl	<dl	<dl	<dl	<dl	<dl	<dl
P2O5	<dl	<dl	<dl	<dl	0.01	<dl	<dl	<dl	<dl
Total	93.96	95.43	95.12	95.5	94.74	94.87	94.49	94.79	93.47
Structural formula on the basis of 4 oxygen atoms									
Si	0.004	0.002	0.002	0.003	0.002	0.002	0.005	0.008	0.003
Ti	0.002	0.005	0.002	0.001	0.003	0.001	0.002	0.001	0.001
Al	0.003	0.004	0.002	0.002	0.005	0.004	0.002	0.002	0.002
Fe+3	1.861	1.801	1.865	1.864	1.781	1.826	1.844	1.874	1.892
Fe+2	0.984	0.981	0.985	0.985	0.977	0.982	0.986	0.993	0.986
Mn	0.007	0.010	0.005	0.004	0.012	0.006	0.008	0.004	0.004
Mg	0.012	0.013	0.011	0.011	0.013	0.011	0.011	0.010	0.011
Ca	0.000	0.000	0.000	0.000	0.000	0.000	0.000	0.000	0.000
Na	0.001	0.000	0.001	0.000	0.000	0.001	0.000	0.000	0.000
K	0.000	0.000	0.000	0.000	0.000	0.000	0.000	0.000	0.000
Cr	0.119	0.176	0.121	0.122	0.200	0.159	0.134	0.101	0.093
Ni	0.011	0.011	0.010	0.010	0.010	0.011	0.011	0.011	0.011
Mol % Usp *Stormer (1983)*	0.00	0.01	0.00	0.00	0.00	0.00	0.00	0.00	0.00

APPENDIX 5

Chemical composition of ilmenite in the chloritite

Sample No.	Br19													CHL5				
Spot No.	**Ilm1**	**Ilm2**	**Ilm3**	**Ilm4**	**Ilm5**	**Ilm6**	**Ilm7**	**Ilm8**	**Ilm9**	**Ilm10**	**Ilm11**	**Ilm12**	**Ilm13**	**Ilm1**	**Ilm3**	**Ilm6**	**Ilm8**	**Ilm9**
SiO2	0.03	0.02	0.03	0	0.02	0.04	0.03	0.02	0.01	0.04	0.06	0.13	0.24	<dl	0.01	0.01	0.01	0.02
TiO2	50.2	49.91	49.99	50.08	49.89	50.3	49.76	49.84	49.83	50.13	49.78	49.85	49.67	52.03	50.38	51.71	49.77	50.75
Al2O3	0.01	<dl	0.01	<dl	<dl	0.01	<dl	0.01	<dl	0.01	0.03	0.05	0.11	0.01	<dl	<dl	0.01	0.01
Cr2O3	0	0.01	0.01	0.02	0.01	0.01	<dl	<dl	<dl	<dl	<dl	<dl	<dl	<dl	<dl	<dl	<dl	<dl
FeO*	40.01	43.33	41.88	40.65	42.92	41.84	41.85	42.78	40.66	41.26	40.51	40.8	39.1	38.48	36.67	42.65	42.54	38.05
MnO	7.78	3.78	6.05	6.14	3.96	5.92	4.52	4.08	5.88	6.11	6.72	6.53	9.03	9.33	12.43	4.23	7.03	10.73
MgO	0.02	0.04	0.04	0.04	0.03	0.02	0.02	0.02	0.02	0.03	0.01	0.01	<dl	0.02	0.02	0.02	0.02	0.02
NiO	0.01	0.02	0.02	<dl	<dl	0.02	0.01	<dl	<dl	0.01	<dl	0.01	0.01	0.02	0.02	<dl	0.01	0.03
CaO	0.05	0.03	0.05	0.05	0.04	0.07	0.04	0.05	0.09	0.03	0.24	0.1	0.09	0.04	0.02	0.01	0.04	0.04
Na2O	0.04	0.06	0.03	0.11	0.09	0.05	0.12	0.1	0.11	0.08	0.07	0.06	<dl	0.01	<dl	0.01	0.02	<dl
K2O	0.01	<dl	0.01	0.01	0.01	0.01	<dl	<dl	0.01	0.02	0.02	0.01	0.02	<dl	0.01	<dl	<dl	0.01
P2O5	<dl	0.01	<dl	<dl	<dl	0.01	<dl	<dl	<dl	<dl	0.03	0.03	0.03	<dl	<dl	<dl	<dl	<dl
Totals	98.16	97.21	98.12	97.1	96.97	98.3	96.35	96.9	96.61	97.72	97.47	97.58	98.3	99.94	99.56	98.64	99.45	99.66
Structural formula on the basis of 3 oxygen atoms																		
Si	0.001	0.001	0.001	0.000	0.001	0.001	0.001	0.001	0.000	0.001	0.002	0.003	0.006	0.000	0.000	0.000	0.000	0.001
Ti	0.969	0.973	0.965	0.978	0.975	0.970	0.979	0.975	0.978	0.972	0.967	0.968	0.956	0.987	0.957	0.995	0.947	0.964
Al	0.000	0.000	0.000	0.000	0.000	0.000	0.000	0.000	0.000	0.000	0.001	0.002	0.003	0.000	0.000	0.000	0.000	0.000
Fe+3	0.060	0.051	0.067	0.042	0.046	0.057	0.038	0.047	0.042	0.052	0.060	0.055	0.073	0.026	0.084	0.010	0.105	0.070
Fe+2	0.798	0.889	0.831	0.840	0.887	0.840	0.878	0.884	0.845	0.838	0.815	0.825	0.764	0.786	0.690	0.902	0.795	0.733
Mn	0.169	0.083	0.131	0.135	0.087	0.128	0.100	0.090	0.130	0.133	0.147	0.143	0.196	0.199	0.266	0.092	0.151	0.229
Mg	0.001	0.002	0.002	0.002	0.001	0.001	0.001	0.001	0.001	0.001	0.000	0.000	0.000	0.001	0.001	0.001	0.001	0.001
Ca	0.001	0.001	0.001	0.001	0.001	0.002	0.001	0.001	0.003	0.001	0.007	0.003	0.002	0.001	0.001	0.000	0.001	0.001
Na	0.002	0.003	0.001	0.006	0.005	0.002	0.006	0.005	0.006	0.004	0.004	0.003	0.000	0.000	0.000	0.000	0.001	0.000
K	0.000	0.000	0.000	0.000	0.000	0.000	0.000	0.000	0.000	0.001	0.001	0.000	0.001	0.000	0.000	0.000	0.000	0.000
Ni	0.000	0.000	0.000	0.000	0.000	0.000	0.000	0.000	0.000	0.000	0.000	0.000	0.000	0.000	0.000	0.000	0.000	0.001
Mol % Ilm Stormer (1983)	0.97	0.97	0.96	0.98	0.98	0.97	0.98	0.98	0.98	0.97	0.97	0.97	0.96	0.99	0.95	0.99	0.94	0.96

APPENDIX 6

Chemical composition of brookite and ferritchromite in the chloritite

Mineral	**Brookite**												**Ferritchromite**					
Sample No.	**Br19**					**CHL5**							**Br19**			**CHL**		
Spot No.	**Bro1**	**Bro2**	**Bro3**	**Bro4**	**Bro5**	**Bro1**	**Bro2**	**Bro3**	**Bro4**	**Bro5**	**Bro6**	**Bro7**	**F-Cr1**	**F-Cr2**	**F-Cr3**	**F-Cr4**	**F-Cr5**	**F-Cr6**
SiO2	0.19	0.13	0.04	0.12	0.18	0.26	0.04	0.18	0.04	0.18	0.07	0.22	0.01	0.01	0.08	0.02	0.05	0.04
TiO2	57.96	58.14	47.92	50.14	56.26	57.53	61.37	56.76	48.51	59.41	53.69	50.87	0.48	0.49	0.63	0.42	0.65	0.54
Al2O3	0.1	0.1	0.03	0.08	0.13	0.19	0.02	0.1	0.03	0.12	0.05	0.14	0.51	0.54	0.82	0.41	0.83	0.62
Cr2O3	<dl	0.02	<dl	0.02	0.01	0.03	<dl	<dl	<dl	0.02	0.01	<dl	30.84	30.09	39.11	26.14	40.55	32.64
FeO*	35.21	34.52	44.26	43.13	36.51	35.87	33.61	36.9	44.69	33.61	38.59	40.85	61.99	62.55	53.12	66.57	51.86	59.95
MnO	0.35	0.64	1.02	1.26	0.36	0.14	0.41	0.53	0.72	0.3	0.94	0.69	1.97	1.91	2.39	1.68	2.51	2.06
MgO	0.14	0.12	0.02	0.07	0.09	0.18	0.03	0.12	0.02	0.12	0.04	0.14	0.56	0.58	0.8	0.51	0.78	0.64
NiO	0.02	<dl	<dl	0.02	<dl	<dl	<dl	0.02	0.01	<dl	0.01	0.01	0.19	0.21	0.18	0.25	0.14	0.19
CaO	0.09	0.13	0.23	0.03	0.16	0.19	0.22	0.05	0.15	0.29	0.05	0.09	<dl	<dl	<dl	<dl	<dl	<dl
Na2O	0.02	0.04	<dl	0.01	0.02	0.04	0.03	<dl	<dl	0.04	0.01	0.01	0.02	0.04	0.03	0.03	0.04	0.03
K2O	0.01	<dl	<dl	0.05	0.01	0.04	0.01	<dl	<dl	0.01	0.03	<dl	<dl	<dl	<dl	<dl	<dl	<dl
P2O5	0	<dl	<dl	<dl	0.02	0.02	<dl	<dl	<dl	0.01	<dl	0.01	<dl	<dl	<dl	<dl	<dl	<dl
Total	94.09	93.84	93.52	94.93	93.75	94.49	95.74	94.66	94.17	94.11	93.49	93.03	96.57	96.42	97.16	96.03	97.41	96.71
	Structural formula on the basis of 3 oxygen atoms												Structural formula on the basis of 4 oxygen atoms					
Si	0.005	0.004	0.001	0.003	0.005	0.007	0.001	0.005	0.001	0.005	0.002	0.006	-	-	-	-	-	-
Ti	1.179	1.187	0.972	1.002	1.148	1.165	1.233	1.146	0.977	1.212	1.096	1.039	0.014	0.014	0.018	0.012	0.018	0.015
Al	0.003	0.003	0.001	0.003	0.004	0.006	0.001	0.003	0.001	0.004	0.002	0.004	0.023	0.024	0.036	0.018	0.037	0.027
Fe+3	-	-	-	-	-	-	-	-	-	-	-	-	1.034	1.053	0.771	1.178	0.729	0.974
Fe+2	1.170	1.171	0.949	0.974	1.141	1.161	1.223	1.133	0.961	1.205	1.074	1.023	0.914	0.914	0.892	0.922	0.891	0.908
Mn	0.008	0.015	0.023	0.028	0.008	0.003	0.009	0.012	0.016	0.007	0.022	0.016	0.063	0.061	0.076	0.054	0.079	0.065
Mg	0.006	0.005	0.001	0.003	0.004	0.007	0.001	0.005	0.001	0.005	0.002	0.006	0.031	0.033	0.045	0.029	0.043	0.036
Ca	0.001	0.000	0.000	0.001	0.000	0.000	0.000	0.001	0.000	0.000	0.000	0.000	-	-	-	-	-	-
Na	0.005	0.007	0.012	0.002	0.008	0.010	0.011	0.003	0.008	0.015	0.003	0.005	-	-	-	-	-	-
K	0.001	0.001	0.000	0.000	0.001	0.001	0.001	0.000	0.000	0.001	0.000	0.000	-	-	-	-	-	-
Cr	0.000	0.000	0.000	0.001	0.000	0.001	0.000	0.000	0.000	0.000	0.001	0.000	0.916	0.895	1.157	0.780	1.198	0.969
Ni	0.000	0.000	0.000	0.000	0.000	0.000	0.000	0.000	0.000	0.000	0.000	0.000	0.006	0.006	0.005	0.008	0.004	0.006

APPENDIX 7

Chemical composition of epidote in the chloritite

Sample No.	Br19										Chl5								
Rock type	**Epi1**	**Epi2**	**Epi3**	**Epi4**	**Epi5**	**Epi6**	**Epi7**	**Epi8**	**Epi9**	**Epi10**	**Epi2**	**Epi3**	**Epi4**	**Epi7**	**Epi8**	**Epi9**	**Epi10**	**Epi11**	**Epi12**
SiO2	38.09	37.74	38.1	37.45	37.48	37.86	38.05	38.04	38.53	38.24	37.75	37.91	37.47	37.87	38.25	37.94	38.73	37.65	38.51
TiO2	0.14	0.12	0.23	0.09	0.12	0.14	0.16	0.07	0.08	0.14	0.1	0.13	0.12	0.18	0.08	0.13	0.11	0.13	0.08
Al2O3	24.56	24.36	24.02	24.86	24.31	26.04	24.8	24.29	25.82	27.74	24.9	24.19	24.35	25.77	25.46	24.92	25.86	24.29	26.62
Cr2O3	0.01	0.01	0.01	0.01	<dl	0.02	0.01	0.01	0.02	<dl	0.08	0.01	0.01	0.01	<dl	0.01	0.03	0.07	0.01
FeO*	10.45	10.89	10.91	10.26	10.66	8.7	10.43	10.88	9.12	6.5	10.71	10.94	10.7	8.83	9.72	10.18	9.75	10.99	8.2
MnO	0.17	0.25	0.23	0.28	0.26	0.16	0.22	0.23	0.17	0.14	0.22	0.21	0.26	0.21	0.24	0.24	0.22	0.26	0.24
MgO	0.01	0.01	0.02	0.04	0.02	0.03	0.02	0.01	0.07	0.04	0.11	0.02	0.04	0.17	0.05	0.02	0.1	0.02	0.08
NiO	<dl	<dl	<dl	<dl	0.01	<dl	<dl	<dl	<dl	<dl	<dl	<dl	<dl	<dl	0.01	<dl	0.02	<dl	<dl
CaO	23.51	23.36	23.28	23.39	23.21	23.68	23.5	23.11	23.57	24.18	23.03	23.39	23.33	23.6	23.25	23.44	23	23.19	23.62
Na2O	<dl	0.01	<dl	<dl	0.01	<dl	0.01	0.01	0.01	0.01	0.01	0.01	0.01	0.03	0.01	0.01	0.01	0.01	0.01
K2O	0.01	<dl	0.01	0.01	0.01	0.01	0.01	0.01	0.01	0.02	0.02	<dl	0.01	0.01	0.02	0.01	0.01	0.02	0.03
P2O5	0.02	0.05	0.02	0.02	0.03	0.04	0.04	0.03	0.03	0.09	0.04	0.03	0.03	0.01	0.03	0.04	0.05	0.03	0.08
Total	97.02	96.83	96.86	96.44	96.15	96.71	97.27	96.69	97.46	97.12	97.01	96.88	96.34	96.71	97.14	96.96	97.89	96.7	97.5
Structural formula on the basis of 12 oxygen atoms																			
Si	2.777	2.752	2.775	2.751	2.755	2.793	2.767	2.773	2.811	2.839	2.747	2.762	2.749	2.793	2.791	2.771	2.799	2.748	2.821
Ti	0.010	0.010	0.010	0.000	0.010	0.010	0.010	0.000	0.000	0.010	0.010	0.010	0.010	0.010	0.000	0.010	0.010	0.010	0.000
Al	2.110	2.090	2.060	2.150	2.100	2.260	2.120	2.090	2.220	2.430	2.130	2.080	2.100	2.240	2.190	2.140	2.200	2.090	2.300
Fe(iii)	1.270	1.330	1.330	1.260	1.310	1.070	1.270	1.320	1.110	0.810	1.300	1.330	1.310	1.090	1.180	1.240	1.180	1.340	1.000
Mn	0.010	0.015	0.014	0.017	0.016	0.010	0.014	0.014	0.011	0.009	0.014	0.013	0.016	0.013	0.015	0.015	0.013	0.016	0.015
Mg	0.001	0.001	0.002	0.004	0.002	0.003	0.002	0.001	0.008	0.004	0.012	0.002	0.004	0.019	0.005	0.002	0.011	0.002	0.009
Ca	1.837	1.825	1.817	1.841	1.828	1.871	1.831	1.805	1.843	1.924	1.796	1.826	1.834	1.865	1.818	1.834	1.781	1.813	1.854
Na	0.000	0.001	0.000	0.000	0.001	0.000	0.001	0.001	0.001	0.001	0.001	0.001	0.001	0.004	0.001	0.001	0.001	0.001	0.001
K	0.001	0.000	0.001	0.001	0.001	0.001	0.001	0.001	0.001	0.002	0.002	0.000	0.001	0.001	0.002	0.001	0.001	0.002	0.003
P	0.001	0.003	0.001	0.001	0.002	0.002	0.002	0.002	0.002	0.006	0.002	0.002	0.002	0.001	0.002	0.002	0.003	0.002	0.005

APPENDIX 8

Chemical composition of apatite in the chloritite

Sample No.	Br19								CHL5		
Spot No.	**Apt1**	**Apt3**	**Apt4**	**Apt5**	**Apt6**	**Apt7**	**Apt8**	**Apt10**	**Apt1**	**Apt2**	**Apt3**
SiO2	0.75	0.77	0.63	0.68	1.09	0.75	0.75	0.52	0.05	0.01	0.01
TiO2	0.05	0.07	0.07	0.04	0.13	0.08	0.03	0.07	<dl	0.01	0.02
Al2O3	<dl	<dl	<dl	<dl	0.07	<dl	<dl	0.01	0.03	<dl	<dl
Cr2O3	0.05	0.08	0.05	0.03	0.06	0.08	0.05	0.03	<dl	<dl	<dl
FeO*	0.5	0.95	0.51	0.71	1.39	1	0.48	0.68	0.29	0.06	0.15
MnO	0.12	0.12	0.11	0.12	0.18	0.15	0.1	0.13	0.08	0.06	0.06
MgO	0.02	0.04	0.03	0.05	0.04	0.06	0.03	0.02	0	0.01	0.01
NiO	0.04	0.02	0.03	0.03	0.03	0.02	0.03	0.03	0.01	<dl	<dl
CaO	54.96	54.33	54.68	54.83	54.05	54.37	54.91	55.16	56.49	56.83	57.44
Na2O	0.1	0.16	0.14	0.16	0.16	0.2	0.11	0.11	0.04	0.02	0.03
K2O	0.02	0.02	0.02	0.03	0.03	0.03	0.02	0.03	<dl	<dl	<dl
P2O5	40.52	40.5	40.33	39.78	40.96	39.66	40.35	41.09	39.85	40.31	40.2
Total	97.13	97.06	96.6	96.46	98.19	96.4	96.86	97.88	96.84	97.31	97.92
Structural formula on the basis of 12 oxygen atoms											
Si	0.612	0.629	0.517	0.561	0.879	0.62	0.614	0.421	0.041	0.008	0.008
Ti	0.03	0.04	0.04	0.02	0.08	0.05	0.02	0.04	0	0.01	0.01
Al	0	0	0	0	0.07	0	0	0.01	0.03	0	0
Cr	0.03	0.05	0.03	0.02	0.04	0.05	0.03	0.02	0	0	0
Fe	0.341	0.649	0.35	0.49	0.938	0.691	0.329	0.461	0.2	0.041	0.102
Mn	0.083	0.083	0.077	0.084	0.123	0.105	0.069	0.089	0.056	0.042	0.042
Mg	0.024	0.049	0.037	0.062	0.048	0.074	0.037	0.024	0	0.012	0.012
Ni	0.03	0.01	0.02	0.02	0.02	0.01	0.02	0.02	0.01	0	0
Ca	48.078	47.58	48.117	48.495	46.718	48.145	48.185	47.878	49.958	49.916	50.273
Na	0.158	0.254	0.223	0.256	0.25	0.321	0.175	0.173	0.064	0.032	0.048
k	0.021	0.021	0.021	0.032	0.031	0.032	0.021	0.031	0	0	0
P	28.009	28.027	28.043	27.802	27.976	27.751	27.979	28.182	27.848	27.978	27.802

Appendix 8. Cont.

Sample No.	CHL5									
Spot No.	**Apt4**	**Apt5**	**Apt6**	**Apt7**	**Apt8**	**Apt9**	**Apt1**	**Apt12**	**Apt13**	**Apt14**
SiO2	0.04	0.28	0.03	0.02	<dl	0.01	0.18	0.01	<dl	0.01
TiO2	0.02	0.01	0.01	0.01	<dl	<dl	<dl	0.01	0.02	0.02
Al2O3	<dl	0.19	<dl	<dl	<dl	<dl	0.11	<dl	<dl	<dl
Cr2O3	0.01	0.02	0.01	<dl	0.02	0.01	0.01	0.01	0.01	<dl
FeO*	0.29	0.29	0.21	0.41	0.14	0.16	0.35	0.12	0.09	0.19
MnO	0.06	0.06	0.05	0.08	0.06	0.06	0.07	0.06	0.06	0.06
MgO	0.01	0.06	0.01	<dl	0.02	0.01	0.03	0.01	0.01	0.01
NiO	<dl	0.01	<dl	<dl	<dl	<dl	0.01	<dl	<dl	<dl
CaO	57.05	56.54	56.94	57.28	57.11	57.07	56.36	56.95	57.07	57.44
Na2O	0.02	0.06	0.03	0.03	0.03	0.05	0.05	0.02	0.03	0.04
K2O	0.01	0.01	0.01	0.01	<dl	0.01	<dl	<dl	0.01	<dl
P2O5	40.46	40.1	40.09	40.32	40.32	39.79	39.93	40.41	40.13	40.04
Total	97.97	97.63	97.39	98.16	97.7	97.17	97.1	97.6	97.43	97.81
Structural formula on the basis of 12 oxygen atoms										
Si	0.033	0.229	0.025	0.016	0	0.008	0.148	0.008	0	0.008
Ti	0.01	0.01	0.01	0.01	0	0	0	0.01	0.01	0.01
Al	0	0.18	0	0	0	0	0.11	0	0	0
Cr	0.01	0.01	0.01	0	0.01	0.01	0.01	0.01	0.01	0
Fe	0.198	0.198	0.144	0.279	0.096	0.11	0.241	0.082	0.062	0.13
Mn	0.041	0.042	0.035	0.055	0.042	0.042	0.049	0.042	0.042	0.042
Mg	0.012	0.073	0.012	0	0.024	0.012	0.037	0.012	0.012	0.012
Ni	0	0.01	0	0	0	0	0.01	0	0	0
Ca	49.824	49.504	50.069	50.026	50.025	50.378	49.659	49.885	50.153	50.375
Na	0.032	0.095	0.048	0.047	0.048	0.08	0.08	0.032	0.048	0.063
k	0.01	0.01	0.01	0.01	0	0.011	0	0	0.01	0
P	27.922	27.744	27.856	27.826	27.908	27.755	27.801	27.97	2.867	27.748